University of Helsinki
Department of Radiology

Tactile processing in human somatosensory and auditory cortices

Yevhen Hlushchuk

Brain Research Unit
Low Temperature Laboratory,
and Advanced Magnetic Imaging Centre
Helsinki University of Technology

Finnish Graduate School of Neuroscience

ACADEMIC DISSERTATION

To be publicly discussed by permission of the Faculty of Medicine of the University of Helsinki, in the Auditorium F1 at Helsinki University of Technology, on January, 17, at 12 noon.

ISBN 978-952-92-1527-0 (paperback)
ISBN 978-952-10-3662-0 (PDF)

Supervisor:

Professor Riitta Hari
Brain Research Unit
Low Temperature Laboratory
Helsinki University of Technology
Finland

Reviewers:

Professor Risto A. Kauppinen
Chair of Functional Brain Imaging
School of Sport and Exercise Sciences
The University of Birmingham
UK

Professor Juhani V. Partanen
Department of Clinical Neurophysiology
Jorvi Hospital
Finland

Official opponent:

Professor Gian Luca Romani
Institute of Advanced Biomedical Technologies
University of Chieti
Italy

Table of contents

Abbreviations

ACC	Anterior cingulate cortex
AP	Action potential
BOLD	Blood-oxygenation-level-dependent
EEG	Electroencephalography
FMRI	Functional magnetic resonance imaging
GLM	General linear model
HRF	Hemodynamic response function
ISI	Inter-stimulus interval
MEG	Magnetoencephalography
MI	Primary motor cortex
MNI	Montreal Neurological Institute (template space)
MRI	Magnetic resonance imaging
PPC	Posterior parietal cortex
PET	Positron emission tomography
PSP	Postsynaptic potential
PSS	Parietal somatosensory strip
RF	Radiofrequency
SEF	Somatosensory evoked field
SNR	Signal-to-noise ratio
SPM	Statistical parametric mapping
SSA	Supplementary sensory area
SI	Primary somatosensory (cortex)
SII	Secondary somatosensory (cortex)
TE	Time to echo
TR	Time to repeat
VPL	Ventral posterior lateral nucleus (of the thalamus)
VPM	Ventral posterior medial nucleus (of the thalamus)

List of publications

The thesis is based on the following four publications which are referred to in the text by roman numerals I–IV:

I. **Hlushchuk Y**, Forss N, Hari R (2004) Distal-to-proximal representation of volar index finger in human area 3b. *Neuroimage* 21: 696-700.

II. Malinen S, Schürmann M, **Hlushchuk Y**, Forss N, Hari R (2006) Improved differentiation of tactile activations in human secondary somatosensory cortex and thalamus using cardiac-triggered fMRI. *Exp Brain Res* 174: 297-303.

III. Schürmann M, Caetano G, **Hlushchuk Y**, Jousmäki V, Hari R (2006) Touch activates human auditory cortex. *Neuroimage* 30: 1325-1331.

IV. **Hlushchuk Y**, Hari R (2006) Transient suppression of ipsilateral primary somatosensory cortex during tactile finger stimulation. *J Neurosci* 26: 5819-5824.

Contribution of the author

As the principal author in Studies I and IV, I carried out the measurements and data analysis and was responsible for writing the papers and implementing co-authors' suggestions into the text. In Studies III and II, I took part in development of experiment protocols, acquisition and interpretation of the fMRI data, and I contributed actively to writing of the manuscripts.

Abstract

Tactile sensation plays an important role in everyday life. While the somatosensory system has been studied extensively, the majority of information has come from studies using animal models. Recent development of high-resolution anatomical and functional imaging techniques has enabled the non-invasive study of human somatosensory cortex and thalamus.

This thesis provides new insights into the functional organization of the human brain areas involved in tactile processing using magnetoencephalography (MEG) and functional magnetic resonance imaging (fMRI). The thesis also demonstrates certain optimizations of MEG and fMRI methods.

Tactile digit stimulation elicited stimulus-specific responses in a number of brain areas. Contralateral activation was observed in somatosensory thalamus (Study II), primary somatosensory cortex (SI; I, III, IV), and post-auditory belt area (III). Bilateral activation was observed in secondary somatosensory cortex (SII; II, III, IV). Ipsilateral activation was found in the post-central gyrus (area 2 of SI cortex; IV). In addition, phasic deactivation was observed within ipsilateral SI cortex and bilateral primary motor cortex (IV). Detailed investigation of the tactile responses demonstrated that the arrangement of distal-proximal finger representations in area 3b of SI in humans is similar to that found in monkeys (I). An optimized MEG approach was sufficient to resolve such fine detail in functional organization. The SII region appeared to contain double representations for fingers and toes (II). The detection of activations in the SII region and thalamus improved at the individual and group levels when cardiac-gated fMRI was used (II). Better detection of body part representations at the individual level is an important improvement, because identification of individual representations is crucial for studying brain plasticity in somatosensory areas.

The posterior auditory belt area demonstrated responses to both auditory and tactile stimuli (III), implicating this area as a physiological substrate for the auditory-tactile interaction observed in earlier psychophysical studies. Comparison of different smoothing parameters (III) demonstrated that proper evaluation of co-activation should be based on individual subject analysis with minimal or no smoothing.

Tactile input consistently influenced area 3b of the human ipsilateral SI cortex (IV). The observed phasic negative fMRI response is proposed to result from interhemispheric inhibition via trans-callosal connections.

This thesis contributes to a growing body of human data suggesting that processing of tactile stimuli involves multiple brain areas, with different spatial patterns of cortical activation for different stimuli.

1 Introduction

In our everyday interaction with our nearby environment, tactile sensation is essential. Major tactile input comes in via our hands, which serve as primary tools for exploring and manipulating objects and tools. Touch can also be exploited in tasks, normally assigned to other senses, such as Braille tactile reading and facilitation of hearing.

Invasive studies have shown a well-ordered somatotopic arrangement of different body parts in the primary somatosensory cortex (SI) of both monkeys (Woolsey et al., 1942; Merzenich et al., 1978) and humans (Foerster, 1936; Penfield and Boldrey, 1937). Moreover, in monkeys several separate somatotopic maps of the hand have been identified in different cytoarchitectonic areas of SI cortex (Merzenich et al., 1978; Nelson et al., 1980). Unraveling such finely detailed functional organization in somatosensory cortices of humans has been hampered by the paucity of opportunities to directly record responses from the depth of the central sulcus and the lateral sulcus, where considerable parts of the SI and SII cortices are located.

The development of non-invasive brain imaging techniques such as whole-scalp magnetoencephalography (MEG) and functional magnetic resonance imaging (fMRI) has enabled detailed studies on functional organization of the human brain. For example, somatosensory evoked magnetic fields (SEFs), recorded with MEG, can be easily picked up from the human SI and SII cortices (for a review, see Hari and Forss, 1999). FMRI also allows accurate study of subcortical structures.

This thesis focuses on tactile processing in different functional brain areas. Using MEG and fMRI as research tools, body part representations were studied within somatosensory areas, responses to ipsi- and contralateral stimuli were characterized, areas receiving auditory–tactile input were identified, and cardiac-triggered fMRI was used to investigate tactile processing in the SII cortex and thalamus.

2 Background

2.1 Somatosensory system

The somatosensory system has separate subsystems for detecting mechanical and thermal/painful stimuli. The mechanosensory subsystem can be further divided into proprioceptive (mechanical displacements in muscles and joints) and tactile (mechanical touch) components. The following subsections will examine the tactile system in greater detail.

2.1.1 Tactile receptors

The somatosensory system is unique in the sense that the receptors are spread all over the body, in the skin and beneath it. Among numerous types of different somatosensory receptors, high-sensitivity mechanoreceptors are specialized to provide tactile information (about touch, pressure, vibration, and cutaneous tension). These tactile mechanoreceptors can be subdivided into slowly adapting receptors (Merkel's disks and Ruffini's corpuscles), which respond to persistent stimuli, and rapidly adapting receptors (Meissner's and Pacinian corpuscles), which respond to rapid changes such as offsets and onsets of stimuli. Furthermore, Meissner's and Merkel's receptors are located close to the skin surface, and their small receptive fields allow differentiating small spatial differences. On the other hand, Pacinian and Ruffini's receptors are mainly subcutaneous, have large receptive fields and poor spatial resolution (Purves and Williams, 2001).

According to Johnson and colleagues (2000), Merkel's receptors are responsible for form and texture information, Meissner's receptors provide feedback information, required for grip control (sensitive to low-frequency skin motion), Pacinian receptors detect distant events by vibration transmitted through objects and tools, and Ruffini's receptors provide information used for the perception of hand conformation and of forces acting on it.

2.1.2 Tactile afferent pathways

The cell bodies of the first neurons in the afferent tactile pathway are situated in the spinal ganglia, close to the spinal cord. They deliver signals from peripheral mechanoreceptors via the cuneate or gracile fascicle of the dorsal horn to target neurons situated at the brainstem level in cuneate nucleus (upper part of the body) or gracile

nucleus (lower part of the body). The fibers, uncrossed up to this level, cross the body midline in the brainstem within medial lemniscus and reach the ventral posterior lateral (VPL) nucleus of the thalamus. They synapse onto thalamic relay neurons, which deliver information to the SI cortex (mainly to area 3b).

Tactile information from the anterior two thirds of the head is carried through the trigeminal portion of the mechanosensory system. This pathway is also crossed only once, in the medial lemniscus, and its three relay stations reside (i) in the trigeminal ganglion, (ii) the principal nucleus of trigeminal complex, and (iii) in the ventral posterior medial (VPM) nucleus of the thalamus.

It should be noted that a small subset of tactile signals is transmitted via the anterolateral system along with thermal and pain signals (afferent fibers decussate at the spinal level and ascend to VPL within the anterolateral tract on the contralateral side) (Kandel et al., 2000).

2.1.3 Cortical somatosensory areas

SI cortex

The SI cortex receives primary afferent input from the thalamus and is located in the postcentral gyrus of the human brain. Based on cytoarchitectonic characteristics, the SI cortex has been subdivided into 4 areas (Geyer et al., 1999; Grefkes et al., 2001) as depicted in Figure 2.1:

area 3a (occupies mainly the fundus of the central sulcus),
area 3b (occupies the posterior bank of the central sulcus),
area 1 (occupies mostly the crown of the postcentral gyrus),
area 2 (occupies the posterior wall of the postcentral gyrus).

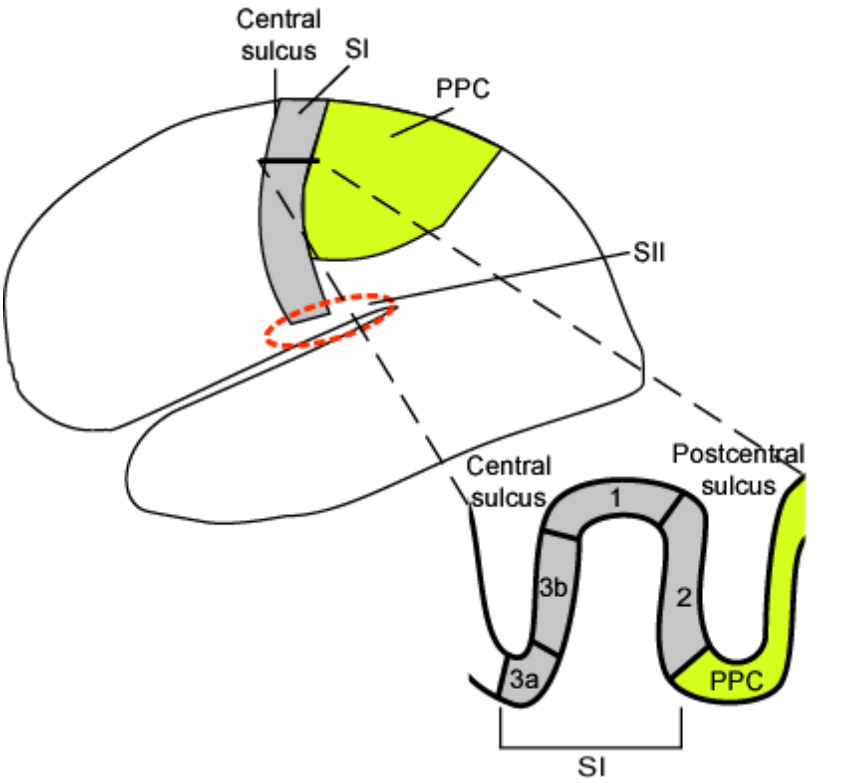

Figure 2.1

Main somatosensory cortex areas (SI, PPC and SII) and cytoarchitectonic subdivisions of the SI cortex, areas 3a, 3b, 2 and 1, are shown in the transverse to the postcentral gyrus cut.

Area 3b mainly receives direct thalamic input, whereas areas 1 and 2 of SI receive main input from area 3b and only minor input from thalamus (Jones and Powell, 1970). Area 3b in monkeys and the SI area described for most mammals have similar cytoarchitectonic structure and orientation of the body maps, and receive major thalamic input from the ventroposterior nucleus. To acknowledge this homology, the term “proper SI” was suggested to distinguish area 3b amongst other areas (3a, 1 and 2) of the SI cortex in monkeys (Merzenich et al., 1978; Kaas et al., 1981).

The areas of the SI cortex also differ by their function: Areas 3b and 1 respond primarily to cutaneous stimuli, whereas area 3a responds mainly to proprioceptive stimuli, and area 2 processes both tactile and proprioceptive stimuli (Powell and Mountcastle, 1959; Hyvärinen and Poranen, 1978; Iwamura et al., 1983a; 1983b, 1993). Within the SI cortex, the complexity of the functional properties of neurons is increasing in the rostro-caudal direction: Simple organization of receptive fields in area 3b, larger, often overlapping receptive fields in area 1, and even more complex receptive fields in area 2 (Hyvärinen and Poranen, 1978; Iwamura et al., 1980; 1983a; 1983b; 1993).

In humans, a similar organization of the SI cortex in the rostro-caudal direction has been confirmed in numerous fMRI studies (Francis et al., 2000; Krause et al., 2001;

Deuchert et al., 2002; Young et al., 2004; Ruben et al., 2006): These studies have demonstrated that in this direction convergence and integration of different tactile inputs lead to progressive blurring of the somatotopy (Young et al., 2004), increased overlap of finger representations (Francis et al., 2000; Kurth et al., 2000; Krause et al., 2001; Deuchert et al., 2002), and greater suppression of multidigit inputs (Ruben et al., 2006).

SII cortex

According to Eickhoff et al. (2006a) the nomenclature for secondary somatosensory cortex (SII) cortex was primarily introduced to describe a second somatotopic representation of cat's feet, found next to the previously described SI cortex (Adrian, 1940). This historical order of discoveries has determined the numbering and naming of the somatosensory cortices: the primary (first) and the secondary (second) somatosensory cortex (Burton and Robinson, 1981). In humans, the SII cortex was detected in the parietal operculum with direct electrical stimulation during epilepsy surgery (Penfield and Jasper, 1954). The first non-invasive recordings of SII activity in humans were obtained with MEG (Hari et al., 1983b; 1984).

The SII cortex responds bilaterally to electrical nerve stimulation (Hari et al., 1983b; 1984; 1993), light touch (Disbrow et al., 2000) and painful stimuli (Hari et al., 1983a; Huttunen et al., 1986; Hari et al., 1997; Ferretti et al., 2003; 2004) and its activity is strongly modulated by tactile attention (Mima et al., 1998).

Recent histological studies on human post-mortem brains have revealed four distinct cytoarchitectonic areas within the SII region (Eickhoff et al., 2006a), whereas in monkeys only three distinct areas have been described (Krubitzer and Kaas, 1990). Comparison with previous functional studies demonstrates that these four cytoarchitectonically defined areas are likely anatomical correlates of the functionally defined SII region in the human parietal operculum (Eickhoff et al., 2006b).

Posterior parietal cortex (PPC)

Another important somatosensory area is the posterior parietal cortex (PPC) which occupies most of lateral parietal cortex not included in SI and SII. In monkeys, the PPC comprises cytoarchitectonic areas 5 and 7, whereas in humans the analogues of these cytoarchitectonic areas occupy only the superior part of the PPC, above the intraparietal sulcus, and human-specific areas 39 and 40 comprise the inferior part of the PPC (Zilles

and Palomero-Gallagher, 2001). Somatosensory evoked responses in the human superior PPC were first recorded with MEG in our laboratory (Forss et al., 1994b).

The PPC is known as “parietal association area” and is considered to integrate tactile and motor processing and to combine these with other sensory information. Its role appears crucial in visual-motor integration and control of visually guided movements (Rizzolatti et al., 1997; Fogassi and Luppino, 2005; Culham and Valyear, 2006; Iacoboni, 2006), perception of personal and peripersonal space, spatial attention (Prado et al., 2005; Culham and Valyear, 2006), and route navigation (Nitz, 2006). The importance of the PPC in space perception is emphasized by such lesion-induced phenomena as spatial neglect and visual, tactile, olfactory or auditory extinction (Vallar, 1998), and optic ataxia (Karnath and Perenin, 2005).

The PPC also belongs to the cerebral network controlling both voluntary and non-voluntary movements (Schnitzler et al., 2006) such as slow voluntary movements (Gross et al., 2002), voluntary (Pollok et al., 2004) and parkinsonian tremor (Timmermann et al., 2003).

Supplementary sensory area (SSA)

Penfield and Jasper (1954) elicited contra- and sometimes bilateral sensations in 2 patients by applying electrical stimulation to the posterior part of mesial parietal cortex which they named a supplementary sensory area (SSA). Recordings in this area in monkeys have revealed neurons with large receptive fields embodying the trunk, face and limbs, but no neurons with receptive fields on the distal proximities (Murray and Coulter, 1981), suggesting that traditionally employed stimulation of distal limbs (such as stimulation of tibial or median nerves) is inadequate for electrophysiological studies of the SSA (Allison et al., 1991). Intraoperative and chronic implant subdural recordings in 47 patients have still failed to reliably localize the SSA within the mesial parietal cortex (Allison et al., 1996).

The function of the SSA still remains vague. Only large lesions of the mesial parietal cortex have caused somatosensory disruption, a pansubmodality somesthetic syndrome. The clinical picture then resembles lesions of the SI cortex (Caselli, 1991), but despite the severity of the disruption, a considerable recovery occurs (Caselli, 1993). The similarity in the clinical picture suggests active interaction between the SI cortex and the SSA, while good recovery suggests somewhat redundant and, hence, well-compensated by other regions role of the SSA in the sensory processing (Caselli, 1993).

2.1.4 Functional organization of tactile processing

Serial vs. parallel processing in SI and SII cortices

In addition to cortico-cortical connections between the SI and SII cortices (Jones and Powell, 1969), monkey studies have revealed that both SI and SII cortices receive direct thalamic input (Jones and Powell, 1970; Stevens et al., 1993), and thalamic neurons projecting to the SI and SII cortices have no "systematic differences in functional capacities" (Zhang et al., 2001b). These findings advocated parallel processing of thalamic input in the SI and SII cortices in primates, as occurs in lower mammals, e.g., cats (Turman et al., 1992). A strong evidence for serial processing in marmosets was obtained, when surgical ablation of the SI cortex resulted in unresponsiveness of SII neurons (Garraghty et al., 1990). These results were later on challenged by Zhang and colleagues (1996; 2001a), who applied reversible cooling ablation of the SI and SII cortices in marmoset monkeys to demonstrate equally independent processing of the sensory input in the SI and SII cortices and, hence, equal hierarchy of the human SI and SII cortices in a parallelly organized network of sensory processing.

In humans, serial processing of tactile input in the SI and SII cortices has been favored by the MEG (Hari et al., 1984; Disbrow et al., 2001; Inui et al., 2004) and intra-cortical potential findings (Frot and Mauguiere, 1999), which have shown later latency of SII responses as compared with early SI responses. Nevertheless, an MEG study on stroke patients has suggested functional independence of tactile processing in the ipsilateral SII cortex to take place under certain circumstances (Forss et al., 1999), despite the considerably later latency of the SII responses. Moreover, an MEG study, exploiting an omitting stimulus paradigm, has favored parallel processing by demonstrating simultaneous early responses in the SI and SII cortices (Karhu and Tesche, 1999). Thus, one might conclude that the position of the human SI and SII cortices in the hierarchy of tactile processing is still under debate.

Body surface maps in SI, SII and thalamus

The anatomical structure of the afferent pathways results in systematically arranged surface body maps in somatosensory cortex. One spinal ganglion receives peripheral input from one dermatome of the body surface (dermatomes can be defined on the basis of this innervation). Thus, axons from a given dermatome gather into a bundle in

a spinal ganglion. These bundles enter the spinal cord at the lateral border of the posterior column and ascend. Consequently, an incoming bundle always occupies the most lateral place in the posterior column, in the immediate vicinity of its entrance into the spinal cord. Such placement results in a strictly defined order of the axon bundles within the posterior column. Such systematic arrangement is preserved throughout the afferent pathway and thalamus, and is observed also at the cortical level. In the SI cortex sacral dermatomes are represented most medially, lumbar and thoracic centrally, cervical dermatomes laterally and trigeminal portion (face) most laterally (Kandel et al., 2000).

Invasive studies have shown such well-ordered somatotopic arrangement of different body parts to exist in the SI cortex of both monkeys (Woolsey et al., 1942; Merzenich et al., 1978) and humans (Foerster, 1936; Penfield and Boldrey, 1937). In humans, this somatotopic arrangement in the medial-lateral direction has been confirmed with different non-invasive methods such as positron emission tomography (PET) (Fox et al., 1987), MEG (Hari et al., 1984; Okada et al., 1984; Baumgartner et al., 1991b; Hari et al., 1993), fMRI (Gelnar et al., 1998; Maldjian et al., 1999), and even scalp electroencephalography (EEG) (Buchner et al., 1995).

Moreover, monkey studies have demonstrated that each of the four cytoarchitectonic areas of the SI cortex contains a separate complete somatotopic map of the body (Merzenich et al., 1978; Nelson et al., 1980; Kaas et al., 1981). Cortical potential recordings in humans are consistent with multiple body representations within the SI cortex. For example, models with multiple (two) sources in the SI cortex robustly explain most of the signal obtained with electrocorticography recordings (Allison et al., 1989b). More recent PET (Burton et al., 1997), MEG (Hashimoto et al., 2001) and fMRI findings (Lin et al., 1996; Gelnar et al., 1998; Kurth et al., 1998; Francis et al., 2000; Kurth et al., 2000; Krause et al., 2001; Deuchert et al., 2002; Blankenburg et al., 2003; Ruben et al., 2006) have unequivocally demonstrated multiple body representations within the human SI cortex.

In addition to the medial-lateral arrangement, in monkeys the body maps in area 3b and 1 are mirror images of each other so that, for example, the proximal phalanges of the fingers are represented close to the common border of areas 3b and 1 and the fingertips are represented further away from the border (Merzenich et al., 1978; Nelson et al., 1980).

To investigate such distal-proximal orientation within cytoarchitectonic areas of the human SI cortex, high resolution non-invasive methods are required. The few MEG studies addressing this issue failed to demonstrate distinct distal-proximal arrangement

within area 3b and thus argued that the representation was smeared or even non-existent in humans (Hashimoto et al., 1999a; 1999b; Druschky et al., 2002). To study whether distal-proximal somatotopic arrangement does exist in human area 3b, in Study I we applied tactile stimuli to the distal and proximal phalanges of the index finger in 11 healthy adults. In comparison with the earlier MEG studies, we recorded cortical responses with a higher resolution whole-scalp neuromagnetometer (I).

Within the human SII region, rough somatotopic arrangement has been observed in numerous MEG (Hari et al., 1993; Del Gratta et al., 2002) and fMRI studies (Del Gratta et al., 2000; Disbrow et al., 2000; Ruben et al., 2001; Ferretti et al., 2003; 2004). Detailed fMRI studies have successfully demonstrated at least 2 distinct somatotopic body maps in the human SII region (Disbrow et al., 2000; Ferretti et al., 2003; 2004).

In the thalamus, crude somatosensory body maps have been identified in neurodegeneration (Jones and Powell, 1970) and neuroanatomical tracing (Krubitzer and Kaas, 1992) studies in monkeys. In the human thalamus, the finger representation has been previously identified with fMRI in the VPL nucleus during stimulation of the palm with a blunt wooden probe in 1-min blocks (Davis et al., 1998). In addition, noxious thermal stimuli elicited fMRI activations in dorsomedial nuclei, and in the VPL (thumb stimuli) or the VPM nucleus (face stimuli) (DaSilva et al., 2002). Thalamic fMRI activations were also observed during self-produced hand, foot and lip movements (Lehericy et al., 1998; Gerardin et al., 2003).

Detection of sensory body maps in the human thalamus creates a real challenge for current non-invasive neuroimaging techniques. First, the investigated structures, thalamic nuclei, are much smaller than, for example, the SI cortex or even its cytoarchitectonic subdivisions, and, hence, particularly high spatial resolution is required. Second, these structures are buried deep within the brain, which makes it difficult to study them with EEG or MEG. FMRI seems a suitable method, as it has high spatial resolution, and the signal is not hampered by the deep position of the thalamus. The fMRI signal is, however, compromised by the presence of large vessels in the vicinity of the thalamus, which increase signal variance due to heart-function-related artifacts (Dagli et al., 1999) and cause movement of the thalamus with the velocity of up to 1.5 mm/s (Poncelet et al., 1992). One possibility to deal with these artifacts is to use cardiac-gated fMRI as was done in the present Study II (see section “Cardiac-gated fMRI” for details).

Plasticity

Sensory body maps are adaptively reorganized to reflect recent experience and learning (Buonomano and Merzenich, 1998; Feldman and Brecht, 2005). For example, in monkey SII cortex, extensive plastic changes take place after surgical elimination of the hand representation in SI: the hand area in SII is occupied by foot representation within 2 months (Pons et al., 1988). Plastic reorganization takes place even within strictly arranged somatotopic maps in areas 3b and 1. For example, after transsection of the median nerve, the cortex previously devoted to the innervated surface has been occupied by neighboring body part representations, without changes in the general somatotopic order (Merzenich et al., 1983).

Neuroimaging studies have successfully documented plastic changes within the human neocortex. For example, an MEG study demonstrated plastic changes within area 3b of SI cortex after surgical separation of fingers in syndactyly patients (Mogilner et al., 1993). An extensive training has also been shown to result in the reorganization of cortical representations (Kelly and Garavan, 2005), e.g., in Braille readers (Pascual-Leone and Torres, 1993) and in musicians (Elbert et al., 1995).

Clearly, knowledge on body part representations is a prerequisite for studying plastic changes, i.e., reorganization of body maps, in somatosensory regions. To reveal body part representations within human somatosensory cortex researchers have successfully employed fMRI, MEG, and high-density EEG (for an extensive review, see Rossini and Pauri, 2000).

Ipsilateral input to SI cortex

In intracranial recordings, area 3b of the human SI cortex is activated only by contralateral tactile stimuli, whereas the more posterior parietal cortex (possibly areas 1, 2, and 5) may display long-latency responses also to ipsilateral activation of the somatosensory afferents (Allison et al., 1989a). Ipsilateral input to the human SI cortex has been suggested by EEG studies dating back to the 1970's (Tamura, 1972), however, such scalp EEG findings disagreed with cortical surface recordings (Allison et al., 1989b) and have been interpreted as volume conductor artifacts (Allison et al., 1991).

In MEG recordings on healthy adults, electric median nerve stimulation elicits long-latency (90–300 ms) responses in the ipsilateral SI region (Korvenoja et al., 1995; 1999). However, such findings are rare: only 13 out of 401 neurological patients and only

1 out of 81 healthy subjects showed ipsilateral 52-ms responses to median nerve stimulation at area 3b (Kanno et al., 2003). Furthermore, not all ipsilateral SI responses do reflect ipsilateral projections: For example, a prominent ipsilateral 58-ms response followed unilateral finger tapping due to tactile contamination, transmitted to the other hand via the table surface (Hari and Imada, 1999).

In fMRI studies, tactile stimuli elicit activations within ipsilateral postcentral sulcus, tentatively in area 2 and/or 5 (Lin et al., 1996; Nihashi et al., 2005). This location coincides with a posterior parietal source demonstrated for air-puff and electric median nerve stimuli in the MEG recordings (Forss et al., 1994b; 1994a; Inui et al., 2004).

Activity changes in the ipsilateral hemisphere have also been reported during unilateral finger movements or low force grip tasks in fMRI recordings (Allison et al., 2000; Nirkko et al., 2001; Hamzei et al., 2002; Stefanovic et al., 2004; Newton et al., 2005). Although these studies typically emphasized deactivation of the ipsilateral primary motor (MI) cortex (Hamzei et al., 2002; Stefanovic et al., 2004; Newton et al., 2005), inspection of the published figures suggests that the deactivation clusters encompassed the ipsilateral SI cortex.

The distinction between MI and SI responses with fMRI might be challenging. Primarily, the confusion between SI and MI cortices could derive from proprioceptive and tactile feedback associated with hand movements and from the anatomical closeness of the SI and MI cortices on the opposite banks of the rolandic sulcus. Moreover, typical spatial smoothing applied in fMRI studies can blur the activations beyond the fragile border. Applying pure tactile stimuli and avoiding spatial smoothing seem to be prerequisites for reliable dissection of SI responses in fMRI studies. Therefore, we applied pure tactile stimuli to fingers of subjects, who kept their hands immobile, to investigate fMRI changes within the contra- and ipsilateral SI cortex in Study IV; to reliably separate MI and SI responses we applied no spatial smoothing in Experiment 2 of Study IV.

Auditory–tactile interaction

The human brain combines all sense information to form percepts of the surrounding environment. Different senses then interact to form a common, more reliable interpretation of an event. An example of interaction between tactile and auditory processing is facilitation of hearing by simultaneous vibrotactile stimuli, both in hearing-impaired and normally hearing subjects (Sherrick, 1984; Weisenberger and Miller, 1987; Levänen et al., 1998; Schürmann et al., 2004). An example of the reverse effect—sound

affecting touch—is the “parchment-skin illusion”, which occurs when accentuation of high frequencies of the sound produced during rubbing palms leads to modification of the tactile percept (Jousmäki and Hari, 1998; Guest et al., 2002).

MEG studies have demonstrated that the auditory–tactile interaction depends on the salience of the stimuli: in the case of more salient tactile stimuli, auditory responses seem suppressed (Gobbele et al., 2003), whereas more salient auditory stimuli result in suppression of SII responses (Lütkenhöner et al., 2002).

In monkeys, neurons responsive to somatosensory stimuli have been found in the postauditory cortex (Robinson and Burton, 1980), likely to correspond to recent findings in the posterior auditory belt area (Schroeder et al., 2001; Fu et al., 2003). In humans, neurophysiological studies have identified candidate anatomical correlates for auditory–tactile interaction. MEG (Lütkenhöner et al., 2002; Gobbele et al., 2003) and fMRI (Foxe et al., 2002) and high-density electric potential recordings (Foxe et al., 2000; Murray et al., 2005) have attributed auditory–tactile interaction to the parietal and temporal operculum, SI cortex, and PPC.

In Study III we hypothesized that psychophysically observed vibrotactile facilitation of hearing (Sherrick, 1984; Weisenberger and Miller, 1987; Levänen et al., 1998; Schürmann et al., 2004) would be reflected in the co-activation of a certain area by vibrotactile and auditory stimuli, indicating parallel input to the area. Our aim was to identify such a region of co-activation and to study whether the co-activation would be different for vibrotactile stimuli *vs.* non-vibratory tactile pressure pulses.

2.2 Brain imaging

2.2.1 Magnetoencephalography (MEG)

History of MEG

The first recordings of human brain’s magnetic activity were done by David Cohen in 1968 (Cohen, 1968), who managed to record alpha-rhythm activity of the visual cortex with an induction coil magnetometer. Due to insufficient sensitivity of such a magnetometer, the signals were averaged time-locked to the simultaneously recorded EEG. Successful measurements of spontaneous brain rhythmic activity, that did not require any noise averaging (Cohen, 1972), were carried out with an ultrasensitive sensor called a SQUID (Superconducting Quantum Interference Device). This type of sensor was

invented by Zimmermann and Silver (1966). Its successful introduction into magnetocardiographic measurements (Zimmerman and Frederick, 1971) was a milestone in the technical development of biomagnetism, including those with neuroscience applications.

The first magnetometers used in biological studies comprised only one SQUID (Cohen, 1972). Multi-channel SQUID magnetometers with the capacity to record magnetic activity at a number of sites could improve localization of the sources and facilitate acquisition by covering a much larger area at a time. In Finland, development of multi-channel SQUID devices for brain research was quite rapid in the 1980's (Kajola et al., 1991) when 4-channel (Ilmoniemi et al., 1984), low-noise 7-channel (Knuutila et al., 1987) and 24-channel SQUID magnetometers (Hämäläinen, 1989; Kajola et al., 1989) were developed.

The development of multi-channel devices culminated in 1992 with the first whole-scalp neuromagnetometer, which was developed by Neuromag Ltd. in the Low Temperature Laboratory, Helsinki University of Technology and contained 122 channels. Accordingly, the first whole-scalp MEG recordings were carried out in Low Temperature Laboratory with that very device (Ahonen et al., 1992). With whole-scalp coverage, the activity in both hemispheres could be recorded simultaneously, and, hence, hemisphere differences could be studied reliably (Mäkelä et al., 1993).

Genesis of brain currents

MEG is based on recording of neuromagnetic signals, i.e., magnetic fields that accompany electrical activity of neurons. Both postsynaptic potentials (PSPs) and action potentials (APs) in neuronal cells are accompanied by magnetic fields. MEG is likely to be differentially sensitive to these fields: First, an AP moves along the cell membrane as a current quadrupole, which can only be distinguished at very close distances, while a PSP forms a current dipole, better detectable at a typical measurement distance. Second, the 1 ms duration of the AP is much shorter than that of the PSP, which lasts for tens of milliseconds and despite its smaller amplitude is assumed to result into a measurable MEG signal, thanks to the effective temporal summation. In contrast, APs are likely to have negligible if any input onto recorded MEG signal. Based on these considerations, MEG has been assumed to reflect mainly the postsynaptic activity in brain tissue (Hari, 1990; Hämäläinen et al., 1993; Hari, 1998).

The magnetic field generated by one neuron is by far too weak to be detected with MEG. Theoretical calculations show that effective summation of 10^5–10^6 simultaneous PSPs is needed in order to produce a measurable MEG signal. Approximations based on either neuronal density of the cortex or intracortical current density agree that already 100–250 mm^2 area of cortex activation can be detected with MEG (Hari, 1990).

Intracellular postsynaptic currents seem to be the primary source of external magnetic fields recorded with MEG, whereas extracellular volume currents generate potential distributions recorded with EEG. The external magnetic flux detected with MEG has been shown to follow the net intracellular postsynaptic currents in combined MEG and EEG recordings (Hari et al., 1980) and later in slice recordings in guinea pig (Okada et al., 1997). Now, when anatomical data on 3-D structure of neuronal cells become available, mathematical models of neuronal cells can be used to gain new insights on the genesis of MEG and EEG signals (Murakami and Okada, 2006).

MEG compared with EEG and fMRI

Whole-scalp MEG is a popular method for imaging brain activity. The main advantage of MEG and EEG over fMRI is the high temporal resolution (under 1 ms). Both MEG and EEG signals are caused by the same primary currents in neurons and represent electrophysiological events at the neuronal population level, whereas fMRI detects local hemodynamic changes, on the basis of which inferences on the neuronal activity are made (see section “Functional magnetic resonance imaging” for details).

A great advancement of MEG was to complement knowledge obtained during many years of EEG research: Temporal characteristics of brain activity were complemented with precise locations of neuronal generators of the observed activity. For instance, neuronal generators of auditory responses in the temporal operculum were first reliably localized with MEG (Hari et al., 1980).

The advantage of MEG over EEG in source localization lies in the transparency of skull and surrounding tissues to the magnetic fields (Grynszpan and Geselowitz, 1973; Cuffin and Cohen, 1979). Because MEG signal is not distorted by inhomogenities of the skull and scalp, MEG resolution appears at least 1/3 better than that of EEG (Cuffin and Cohen, 1979; Cohen and Cuffin, 1983). Superior spatial accuracy of MEG over EEG has been demonstrated in a study on implanted dipoles (Cohen et al., 1990), even despite numerous methodological deficiencies of that experiment disadvantaging MEG (Hari et al., 1991; Williamson, 1991; Hämäläinen et al., 1993).

Before development of MEG, cortex buried in the fissures had been poorly explored, because EEG, while able to record all three orthogonal components of a current source, is dominated by radial sources (Cohen and Cuffin, 1983). On the other hand, radial sources, within an ideal sphere, produce no external magnetic field (Baule and McFee, 1965; Grynszpan and Geselowitz, 1973), and tangential sources (parallel to the sphere surface) produce non-zero external magnetic field. Such orientation selectivity explains MEG's sensitivity to the tangential sources, located mostly in the fissural cortex. A good example of the MEG's sensitivity to neuronal sources in the fissural cortex is the non-invasive recordings of SII responses, first obtained namely with MEG (Hari et al., 1983b).

Surprisingly, a recent modeling study (Liu et al., 2002) has shown better spatial accuracy for EEG, although again under certain assumptions which favored EEG: same signal-to-noise ratio (SNR) for EEG and MEG, same number and positioning of sensors, and, most importantly, same forward problem solution (i.e., head model). In this comparison the last one is crucial as it assumes no errors introduced by the head model, which, at the moment, does not hold for EEG and is the main advantage of MEG: Since the skull and scalp are transparent to magnetic fields only the inner surface of the skull is needed for modeling of a source in MEG. On the other hand, the skull and scalp distort and smear electric potentials, recorded with scalp EEG. Hence, precise EEG modeling necessitates individual realistic multi-compartment head model with known conductivities of brain tissue, cerebrospinal fluid, skull and scalp. As a consequence, a lot of uncertainty is brought by the conductivity of the layers which are normally assumed or approximated.

Another advantage of MEG is that no reference is needed and the interpretation of the data is straightforward, whereas for EEG recording the selection of reference point is crucial. Although certain methods allow presentation of EEG data without a reference, e.g., by calculating surface Laplacians (Nunez, 1989), interpretation of the data remains problematic for several simultaneous sources.

Up-to-date modeling studies (Fuchs et al., 1998; Liu et al., 2002) have concluded that combination of MEG and EEG is better in source localization than any modality alone, stressing the complementary nature of MEG and EEG signals and the benefits of their combination, an idea that has been expressed and discussed in much earlier MEG-related papers (Cohen and Cuffin, 1983, 1987; Baumgartner et al., 1991a; Lopes da Silva et al., 1991).

MEG is used not only in basic brain research, but also in clinical neurophysiology. MEG's accuracy in localizing superficial cortical sources has ensured its employment in

epilepsy diagnostics and presurgical mapping (Hari, 2004). At the same time EEG has an advantage of portability, which makes it more suitable than MEG for continuous patient monitoring (Barkley and Baumgartner, 2003).

2.2.2 Functional magnetic resonance imaging (fMRI)

Basics of MRI

Magnetic resonance imaging (MRI) relies on the behavior of nuclear spins in a strong magnetic field. The main sources of the signal measured in MRI studies are hydrogen nuclei (protons).

In a magnetic field, nuclei precess at characteristic resonance frequency that equals to the product of the gyromagnetic ratio and the magnetic field strength and is called Larmor frequency. Radiofrequency (RF) pulse at this frequency excites nuclei, which absorb the energy of the RF pulse and switch from low-energy state (nuclear spin aligned along the external magnetic field) to high-energy state (nuclear spin aligned against the magnetic field). In addition, the RF excitation pulse brings the nuclei spins to the same phase so that they start to precess about the main magnetic field vector with initial phase coherence. After the offset of the pulse, the coherence between nuclear spins is gradually lost (transverse or T2 relaxation). Nuclear spins also begin to realign with the external magnetic field (longitudinal or T1 recovery) and emit energy (at the same Larmor frequency). The emitted signal is picked up by a receiving RF coil of an MRI scanner, and, on the basis of this signal, an MRI image is reconstructed (Haacke et al., 1999; Huettel et al., 2004).

T1 and T2 relaxation times are the main tissue parameters in MRI imaging. T1 is the parameter that describes recovery of longitudinal magnetization which involves exchange of energy between lattice and spins, whereas T2 describes decay of transverse magnetization caused by spin-spin interactions. T2* is another parameter that describes the decay of transverse magnetization due to spin-spin interactions and local field inhomogenities ($T2^* \leq T2$; $T2^* = T2$ only in ideally homogenous tissues). These parameters are tissue characteristic, which enables achievement of high between-tissue contrast without any external contrast injections, just by manipulating pulse-sequence parameters (presuming tissues' T1 and/or T2* relaxation times do differ).

BOLD fMRI

The term fMRI refers to numerous MRI methods that have been developed to track brain activity. The most common method of fMRI is blood-oxygenation-level-dependent (BOLD) contrast imaging that measures hemodynamic correlates of neuronal responses. It exploits hemoglobin as an endogenous contrast agent, relying on the difference in magnetic properties of oxyhemoglobin (diamagnetic) and deoxyhemoglobin (paramagnetic) (Ogawa et al., 1990). The neuronal activity in a region leads, through different mechanisms, to a local decrease of the concentration of deoxyhemoglobin. Such decrease results in the lengthening of T2* decay time due to smaller local field inhomogenities introduced by paramagnetic deoxyhemoglobin, and, consequently, the signal intensity increases in a T2*-weighted image. Thulborn and colleagues (1982) noted that the magnitude of the described effect is proportional to the square of the static field strength, i.e., the BOLD signal is of larger amplitude and, thus, better detected at strong magnetic fields.

The first BOLD fMRI measurements in humans were published in 1992 (Bandettini et al., 1992; Kwong et al., 1992; Ogawa et al., 1992). Since then, several studies have demonstrated correlation of BOLD signal with neuronal activity. The BOLD signal has been demonstrated to correlate most consistently with the level of neuronal postsynaptic activity reflected in local field potentials (Logothetis et al., 2001; Mukamel et al., 2005; Niessing et al., 2005).

The mentioned studies on correlation of BOLD signal with neuronal activity dealt only with positive BOLD responses (typical BOLD responses, described in the beginning of this section). The interpretation of negative BOLD responses in terms of neuronal activity has been far more challenging because inhibition, like excitation, is an active process with high metabolic costs (Nudo and Masterton, 1986)—and, hence, should also result in positive BOLD response (Jueptner and Weiller, 1995). More recent studies have suggested, however, that BOLD responses are driven not by metabolic costs of neuronal activity but rather by neurotransmitter-related signaling (Attwell and Iadecola, 2002), and their amplitudes depend on calcium influx (Lauritzen, 2005): For example, through the inactivation of calcium channels in cortical pyramidal cells, synaptic inhibition would result in a negative BOLD response.

FMRI studies of human visual cortex have suggested negative BOLD responses to reflect suppression of neuronal activity (Smith et al., 2000; Shmuel et al., 2002). The

negative and positive BOLD responses were, however, spatially adjacent (distances between peaks ranged from 2 to 25 mm; Shmuel et al., 2002). Because of the common blood supply of spatially close brain areas, it was not possible to rule out local hemodynamic mechanisms, uncorrelated with neuronal activity. A more recent study has demonstrated negative BOLD responses in the visual cortex of the hemisphere opposite to that displaying positive BOLD responses (Smith et al., 2004). Such spatial separation excludes local hemodynamic effects as a possible explanation, thereby implying neuronal mechanisms in the generation of negative BOLD responses.

Moreover, recent simultaneous fMRI and intracortical recordings demonstrated tight coupling between negative BOLD response and the decrease of neuronal activity in monkey primary visual (VI) cortex (Shmuel et al., 2006). Exact neurovascular mechanisms underlying this coupling are still to be discovered.

The spatial resolution of fMRI has been limited to millimeters, because most of T2* BOLD signal, especially at fields below 4 tesla, comes not from parenchyma (extravascular component) but from drain veins (intravascular component) (Ogawa et al., 1993; Bandettini and Wong, 1995). For high field strength, methods are now being developed to further improve fMRI resolution at sub-millimeter scale to allow laminar separation of activations within cortex (Duong et al., 2001; Goense and Logothetis, 2006). This should allow investigating functional organization of the cortex at far finer level. New horizons are opening for fMRI applications also in clinical practice (Harel et al., 2006). For instance, tracking functional recovery of stroke patients appears feasible with fMRI, since amplitude of brain activations was shown to correlate with motor recovery (Ward et al., 2006).

Cardiac-triggered fMRI

FMRI can reveal human brain activations with high precision. The accuracy may, however, be impaired by movement and deformation of brain tissue associated with cardiac pulsations. Such artifacts might be particularly important in the studies of brainstem structures (thalamus is a good example), when the expected area of activation is small and voxel size is minimal in order to achieve reasonable spatial resolution. In such cases movements of 1.5 mm amplitude (Poncelet et al., 1992) might become an obstacle.

One possibility to deal with such artifacts is to correct the data after the acquisition, using available records of heart function (Biswal et al., 1996; Glover et al., 2000). Another possibility is to reduce such artifacts by implementing cardiac-triggered

fMRI, i.e., synchronization of the fMRI image acquisition to a certain phase of the cardiac cycle. The latter technique has been successfully applied to diminish the effects of heart-function-related movements in the human cortical and subcortical auditory areas (Guimaraes et al., 1998; Griffiths et al., 2001; Behrens et al., 2003b; Schönwiesner et al., 2003; Krumbholz et al., 2005), as well as in the superior colliculus (DuBois and Cohen, 2000).

In cardiac-gated fMRI, acquisition of each volume is time-locked to the cardiac trigger, which means that varying heart rate leads to varying time between acquisitions of consequent volumes (time-to-repetition; TR). Variation of TR results in varying residual longitudinal magnetization (T1) effects and, consequently, in signal intensity fluctuations that might easily exceed the amplitude of BOLD response. Thus, certain signal intensity variations due to unstable TR have to be corrected for (Guimaraes et al., 1998), and different methods have been applied successfully to this end (Guimaraes et al., 1998; DuBois and Cohen, 2000; Behrens et al., 2003b).

3 Aims of the Study

The thesis aims to deepen our knowledge of tactile processing in the human brain by investigating:

- Distal–proximal index finger representation in area 3b of the SI cortex (Study I)
- Somatotopy in the SII cortex and thalamus using cardiac-triggered fMRI, expected to improve detection of tactile activations in the thalamus and SII region where BOLD signal is affected by cardiac-pulse-related movement (Study II)
- Brain areas involved in auditory–tactile interaction (Study III)
- SI and SII responses to tactile stimuli at different frequencies (Experiment 1 of Study IV)
- SI responses to ipsi- and contralateral tactile stimuli (Experiment 2 of Study IV).

4 Materials and Methods

4.1 Subjects

All experiments were carried out on healthy subjects. The experimental protocols had received prior approval by the ethics committee of Helsinki and Uusimaa Hospital District, and informed consent was obtained from all subjects before the experiment. Altogether, 50 healthy subjects took part in the experiments.

The following table gives an overview of the subjects in each study separately.

Study	N	Male/Female	Mean Age (years)	Age Range (years)
I	11	4/7	30	23–43
II	10	6/4	24	20–32
III	13	9/4	28	22–39
IV *Expt.1*	10	7/3	27	23–33
IV *Expt.2*	10 (4 common)	5/5	29	24–45

4.2 Stimuli

In all studies, tactile stimuli were delivered by balloon diaphragms driven by compressed air (Mertens and Lütkenhöner, 2000). In Studies I, II and IV, the tactile stimuli were delivered to the volar surface of the right hand fingers, or to both left and right hand fingers (but never simultaneously; Experiment 2, Study IV). In Study II, tactile stimuli were delivered to lips, right-hand fingers and right toes. Although the stimulus intensity was kept equal for all stimulation sites in Study II, subjects perceived the touch best in the fingers and toes and often weaker in the lip.

In Study III, auditory and vibratory stimuli were also used. Auditory stimuli were bursts of white noise delivered through stereo headphones. Sound intensity was adjusted so that subjects could clearly hear the sounds despite the fMRI scanner noise.

Vibration stimuli were generated with a vibrotactile stimulator (Levänen et al., 1998) via two silicon tubes (diameter 29 mm). The tubes were placed to the left and right from the subject while (s)he was lying in the magnet bore. Only the right tube was in contact with the subject's body. The subject was touching the tube with the right hand so as to maximize finger-to-tube contact, yet with a comfortable relaxed position for the hand.

In all experiments, the subjects were asked to remain vigilant throughout the measurement and attend to the stimuli.

4.3 MEG recordings and data analysis

In Study I, somatosensory evoked fields (SEFs) were recorded with a 306-channel whole-scalp neuromagnetometer (Vectorview, Neuromag, Helsinki, Finland) that contains 102 identical triple sensors, each housing two orthogonal planar gradiometers and one magnetometer.

The exact position of the head with respect to the sensors is needed for source localization. For this purpose, 4 small coils were placed to different sites on the scalp and magnetic signals produced by currents led into those coils were measured. Prior to this measurement, the precise locations of the coils with respect to anatomical landmarks on the scalp were determined with a three-dimensional digitizer to allow alignment of the MEG and MRI coordinate systems. In our head-coordinate system, *x*-axis passed from the left to the right preauricular point, *y*-axis (orthogonal to *x*) went forward through the nasion, and *z*-axis went upwards orthogonal to the *xy* plane. Anatomical head images were obtained for most of the MEG subjects by GE Signa™ 3T device and for some by Siemens MAGNETOM™ 1.5T device.

The signals were filtered with a passband of 0.03–200 Hz and digitized at 1 kHz. The analysis epoch of 400 ms included a prestimulus period of 70 ms. Epochs coinciding with signals exceeding 300 μV in the simultaneously recorded vertical and horizontal electro-oculograms were automatically rejected from the analysis. At least 400 single responses were averaged for each stimulus.

For source identification, the signals recorded by the 204 gradiometers were analyzed. The head was assumed to be a sphere, the dimensions of which were found from individual MRI images. Equivalent current dipoles (ECDs) were used to model sources of local cerebral activations. Only dipoles with goodness-of-fit value ≥ 85%, confidence volume ≤ 1 cm3, and source strength ≥ 5 nAm were accepted for further analysis. An ECD that best explained the first major deflection of the response (judged from comparison between modeled and measured waveforms) was found by a least-squares search using a selection of 24–32 channels in the area of the maximum response. The procedure resulted in the location, orientation, and strength of the ECD in a spherical conductor model. The obtained ECDs were overlaid onto individual MRI images to verify source locations with respect to anatomical structures.

Statistical significance was evaluated using paired, two-tailed *t* tests.

4.4 FMRI recordings and data analysis

Functional MRI was performed on a Signa™ 3T MR scanner (GE Medical systems) using a gradient-echo planar imaging sequence (II, III, IV). In Studies II–IV, a standard head coil was used for imaging. In Experiment 2 of Study IV, the same MRI system, including an EXCITE™ upgrade, was used with an 8-channel head coil. The whole brain was covered with axial-oblique slices in the fMRI measurements except for Study II when the imaged area covered mainly thalamus and SII region. Structural T1 images were obtained in the same recording session with fMRI images.

The acquired fMRI data in Study IV were analyzed with BrainVoyager QX™ (BV QX) software (Brain Innovation B.V., Maastricht, Netherlands). In Studies III and II the analysis was performed with statistical parametric mapping (SPM), namely software packages SPM99 (III) and SPM2 (II) (Wellcome Department of Imaging Neuroscience, London, UK, http://www.fil.ion.ucl.ac.uk/spm).

In all fMRI runs, the first four acquired volumes were omitted from the statistical analysis to include only volumes with full magnetic saturation. Preprocessing of the fMRI data included 3D motion correction, high-pass filtering and linear trend removal. Gaussian spatial smoothing (FWHM = 6 or 8 mm) was used in all studies but Expt. 2 of Study IV, when it could impair distinction between activations in the anterior and posterior bank of the central sulcus, i.e., between the MI and SI cortices.

After preprocessing, the (f)MRI data were normalized to Talairach space (Talairach and Tournaux, 1988) in BVQX and to MNI (Montreal Neurological Institute) space (Evans et al., 1993) in SPM. Further statistical analysis of the normalized data included numerous steps, starting with general linear model (GLM) analysis of individual data. The predictors used in the GLM analysis were obtained by convolving a stimulation time course with the hemodynamic response function (HRF) (Friston et al., 1994; Boynton et al., 1996). First, individual data were analyzed and the resulting individual contrast images were then subjected to random-effects analysis at the group level. At the group level, the contrast images underwent 2-tailed t-tests in BVQX and 1-tailed in SPM (default features). The obtained statistical maps were then thresholded at an appropriate p- or t-value and minimum cluster size (exact numbers are stated separately for each displayed map). Correction for multiple comparisons, if any, was done by applying false discovery rate (Genovese et al., 2002) in BV QX, and by applying cluster corrected thresholding in SPM (Study III).

5 Experiments

5.1 Fingertip and the base of the index finger are only 3 mm apart in area 3b (Study I)

5.1.1 Experimental setup

Tactile stimuli were delivered to the volar skin of the index finger (distal and proximal phalanges) of the (dominant) right hand. Stimulus intensity was adjusted to produce clear tactile sensation and was kept identical for all subjects. The stimuli were presented in a pseudorandom order every 483 ms to one site at a time and no site was stimulated twice in succession.

5.1.2 Results

In all subjects distal and proximal stimuli elicited responses in the left rolandic area. Due to the relatively short inter-stimulus interval (ISI), no systematic activation was observed elsewhere. The responses were stronger to the distal than proximal stimuli in 7 out of 11 subjects, and the main deflections were double-peaked in 9/11 subjects. The earlier deflection peaked at 55 ± 2 ms for distal and at 51 ± 2 ms for proximal stimuli (nonsignificant difference; p = 0.2).

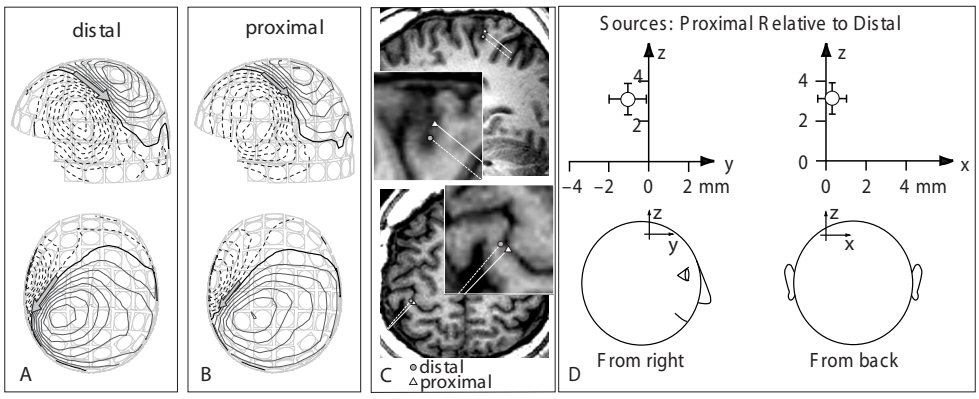

Figure 5.1 Study I

Magnetic field patterns of responses to distal (A) and proximal (B) stimuli in Subject 7 (upper part—view from the left side; lower part—view from the vertex) at 52 ms, the moment of dipole identification. Magnetic flux out of the head is indicated with solid lines and the flux into the head with dashed lines. The arrow denotes the ECD. (C) Sources superimposed on the subject's MR image, with the source area enlarged on the right. The lines denote the dipole direction, approximately orthogonal to the cortical surface. (D) Relative source locations of responses to proximal stimuli shown in a coordinate system in which each individual's current dipole following distal stimuli was situated in the origin. The mean ± SEM source locations are shown in two orthogonal planes (the head on the right is viewed from the back). Adapted from Hlushchuk Y,

Forss N, Hari R (2004) Distal-to-proximal representation of volar index finger in human area 3b. *Neuroimage* 21: 696-700.

Figures 5.1A and 5.1B show magnetic field patterns for Subject 5: The patterns are nicely dipolar to distal and proximal stimuli at 52 ms and can be adequately explained by single ECDs. Superposition of these sources on the subject's MR image in Fig. 5.1C indicates activation in the posterior bank of the central sulcus, in area 3b of the SI cortex, for both stimulation sites. The sources are within 5 mm of each other, and the source to distal stimuli is deeper than that to proximal ones.

Figure 5.1D compares the relative source locations of responses to proximal vs. distal stimuli in the sagittal *(yz)* and coronal *(xz)* planes at group level (n = 11). The sources were 3.1 ± 0.8 mm ($p < 0.003$) more superior to proximal than to distal stimuli, that is, in the direction of depth within the central sulcus. Such a superior–inferior difference was observed in 9 out of 11 subjects ($p = 0.033$; binomial test), whereas in other directions the source locations did not differ.

5.1.3 Discussion

These results demonstrate a distal-to-proximal arrangement of the index finger representation in area 3b of the human SI cortex with about 3 mm deeper sources for distal than proximal digit stimulation site. In owl monkeys, distance between distal and proximal finger representations is about 1 mm in area 3b, which extends 2.5 mm in the rostrocaudal direction (measured from Fig. 2 of Merzenich et al., 1978). Area 3b's extent of 10–12 mm in humans (measured from Figs. 5, 9, and 11 of Geyer et al., 1999) would scale to a distal–proximal difference of about 4 mm, which makes our estimate of 3 mm quite realistic. Interestingly, a recent fMRI study (Blankenburg et al., 2003), which appeared during the revision of our paper, reported a 4-mm distal–proximal difference in the depth direction, in full agreement with our results and the above considerations.

The failure of previous MEG studies (Hashimoto et al., 1999a; 1999b; Druschky et al., 2002) to detect distal–proximal arrangement of finger representations in SI cortex can be explained by a lower SNR and, in part, by a failure to cover both extrema of a dipolar field pattern in the 37-channel recordings of Druchky et al. (2002). During long recording sessions head movements can also add noise to the data and therefore impair source localization. The short ISI and a reasonable number of stimuli allowed us to collect all the data in a much shorter time than in the previous MEG studies and with better SNR (as estimated from published figures).

5.2 Cardiac-triggered fMRI improves differentiation of tactile activations in human SII cortex and thalamus (Study II)

5.2.1 Experimental setup

For each subject, two different types of fMRI acquisition were used: conventional imaging, with a constant TR (3 s), and cardiac-triggered imaging, time-locked to the pulse of a subject and, hence, with a variable TR (2.500–3.160 s). The subjects received tactile stimuli to fingers, lips, and toes. The stimulus blocks lasted 9 volumes, i.e., 9 x 3 s = 27 s during conventional imaging and 26.1 ± 2.6 s during cardiac-triggered imaging (mean ± SD across 10 subjects), and alternated with 7-volume rest periods (21 s during conventional imaging and 20.4 ± 2.1 s during cardiac-triggered imaging).

For each subject, two additional fMRI runs without stimulation were acquired with TR of 1.5 and 10 s. These runs were necessary for the correction of signal variations caused by the variable TR of the cardiac-triggered runs.

5.2.2 Results

Thalamus

Group analysis revealed responses in the posterior part of the thalamus, in areas corresponding to the VPL nucleus, which were specific to finger stimuli and were visible only with cardiac-triggered imaging (left image in the top row of Fig. 5.2). With conventional imaging, statistically significant activations in the thalamus were not observed.

Single-subject analysis revealed statistically significant thalamic activation to finger stimulation in five subjects during cardiac-triggered imaging and in two during conventional imaging. Responses to lip stimulation were seen in two subjects with both methods. Toe stimuli elicited no significant activations in the thalamus.

SII region

Figure 5.2 (top row) shows the group-level activation for finger stimuli during cardiac-triggered imaging. The finger stimuli elicited activation within parietal operculum: one cluster (with 3 local maxima) extending into the depth of the Sylvian fissure in the contralateral (left) hemisphere and 2 separate clusters in the ipsilateral hemisphere. During

conventional imaging (Fig. 5.2, bottom row) the activations were only seen in the contralateral hemisphere.

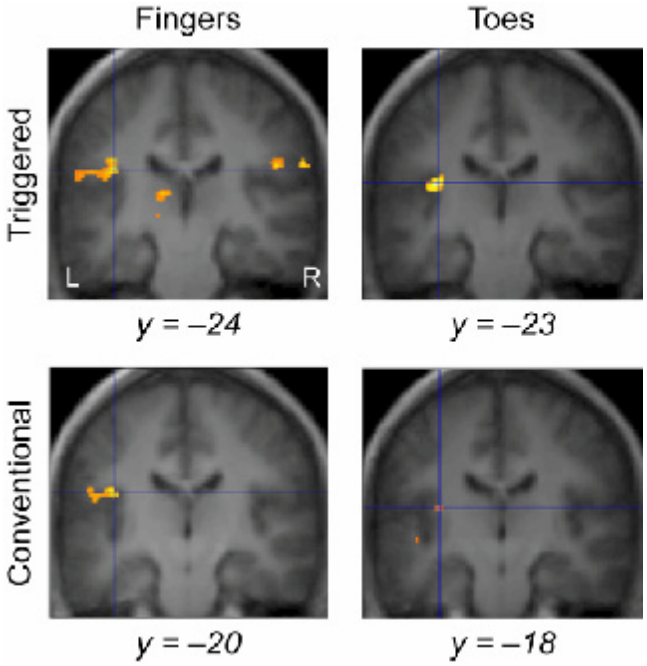

Figure 5.2 Study II

Group-level cortical responses to right finger and toe stimulations during cardiac-triggered (top) and conventional imaging (bottom), overlaid on average anatomical image of ten subjects. L/R, left/right. Adapted from Malinen S, Schürmann M, Hlushchuk Y, Forss N, Hari R (2006) Improved differentiation of tactile activations in human secondary somatosensory cortex and thalamus using cardiac-triggered fMRI. *Exp Brain Res* 174: 297-303 with kind permission of Springer Science and Business Media.

Toe stimulation elicited prominent contralateral activations during conventional and cardiac-triggered imaging. With either imaging method group-level analysis failed to reveal activation clusters for lip stimulation.

Single-subject analysis demonstrated responses to finger stimulation in all ten subjects with both imaging methods in the middle of the lateral sulcus contralateral to stimulation. Medial to these activations, in the fundus of the lateral sulcus, 6/10 subjects showed additional finger responses during cardiac triggering. With conventional imaging, the medial activations were seen only in three subjects.

Contralateral SII responses to toe (lip) stimulation were seen in 8 (6) subjects during cardiac-triggered imaging and in 5 (4) subjects during conventional imaging.

Efficiency of the correction

The statistical significance of the fMRI activation is proportional to the signal change and inversely proportional to the variance of the fMRI signal, and thus both these factors can affect the results. To evaluate the effect of the cardiac-triggering (along with

the applied signal correction) we estimated the signal change (response amplitude) and the signal variance (residual variance after model fitting).

Signals from the selected volumes of interest in cardiac-triggered and conventional imaging were compared in six subjects (total of 12 sessions) who showed both cortical and thalamic responses to finger stimuli. In 5/6 subjects the signal variance was smaller during cardiac-triggered than conventional imaging, and the situation was similar both in the thalamus and SII cortex. Variance decreased statistically significantly ($p < 0.02$) in all conditions, with an average decrease of 26% for thalamic signals, 38% for the medial and 40% for the lateral SII responses. In contrast, signal change between the cardiac-triggered and the conventional fMRI series was statistically insignificant.

5.2.3 Discussion

Cardiac-triggered data acquisition with the applied signal correction improved the detection of touch-related activations both in the thalamus and in the SII region, particularly at the single-subject level. For example, the number of individual subjects, in whom statistically significant activations for finger stimuli were detected, was higher for cardiac-triggered than conventional imaging in the thalamus (5 *vs.* 2) and medial SII cortex (6 *vs.* 3).

The improved detection of activations by cardiac-triggered imaging with post-acquisition correction resulted from the decreased variance of the BOLD signal, without any statistically significant effect on the strength of the BOLD signal. Our results indicate that heart-cycle-related noise can affect the measured signals also at cortical level which is in line with the findings on signal changes during the cardiac cycle near the major blood vessels: In the internal carotid system, strong influences were found bilaterally along the middle cerebral artery, in the superior temporal gyrus and insula, i.e., in the vicinity of the SII region (Dagli et al., 1999). Cardiac-triggered fMRI, together with effective signal correction, can therefore be applied to improve the detection of tactile responses both in the SII cortex and thalamus.

5.3 Touch activates the human auditory cortex (Study III)

5.3.1 Experimental setup

In this study, we used vibrotactile, pulsed-tactile and auditory stimuli in 4 fMRI runs. In 2 runs, vibrotactile stimuli were delivered to the subject's right hand, alternating in

blocks with control vibrations delivered to the tube that was not in contact with the subject. In two other runs pulsed-tactile or auditory stimuli blocks were alternating with stimulus-free rest blocks (only one type of stimulus per run).

5.3.2 Results

Areas activated by vibrotactile, pulsed-tactile and auditory stimuli were obtained through random-effects analysis across 13 subjects, for vibrotactile – control, pulsed-tactile – rest, and auditory – rest contrasts (voxel $p < 0.001$, uncorrected; $p < 0.05$, cluster-corrected).

In group analysis with minimal smoothing (3.1 x 3.1 x 4 mm^3 kernel), auditory stimuli activated the supratemporal auditory cortices bilaterally, up to the auditory belt areas (auditory cortex divisions according to Kaas et al., 1999). Vibrotactile stimuli activated most consistently the left (contralateral) SII cortex, with an extension to the superior temporal gyrus, posterior to the peak voxel of auditory activation. The pulsed-tactile stimuli activated most consistently the left SI and SII cortices, also extending into the superior temporal gyrus, similar to the vibrotactile activation.

Figure 5.3A demonstrates the effect of smoothing on the size of co-activation clusters: with liberal smoothing the total volume of vibrotactile–auditory co-activation was 6.4 times the volume obtained with minimal smoothing; for vibrotactile–auditory co-activation only (without pulsed-tactile activation) the corresponding factor is 4.1.

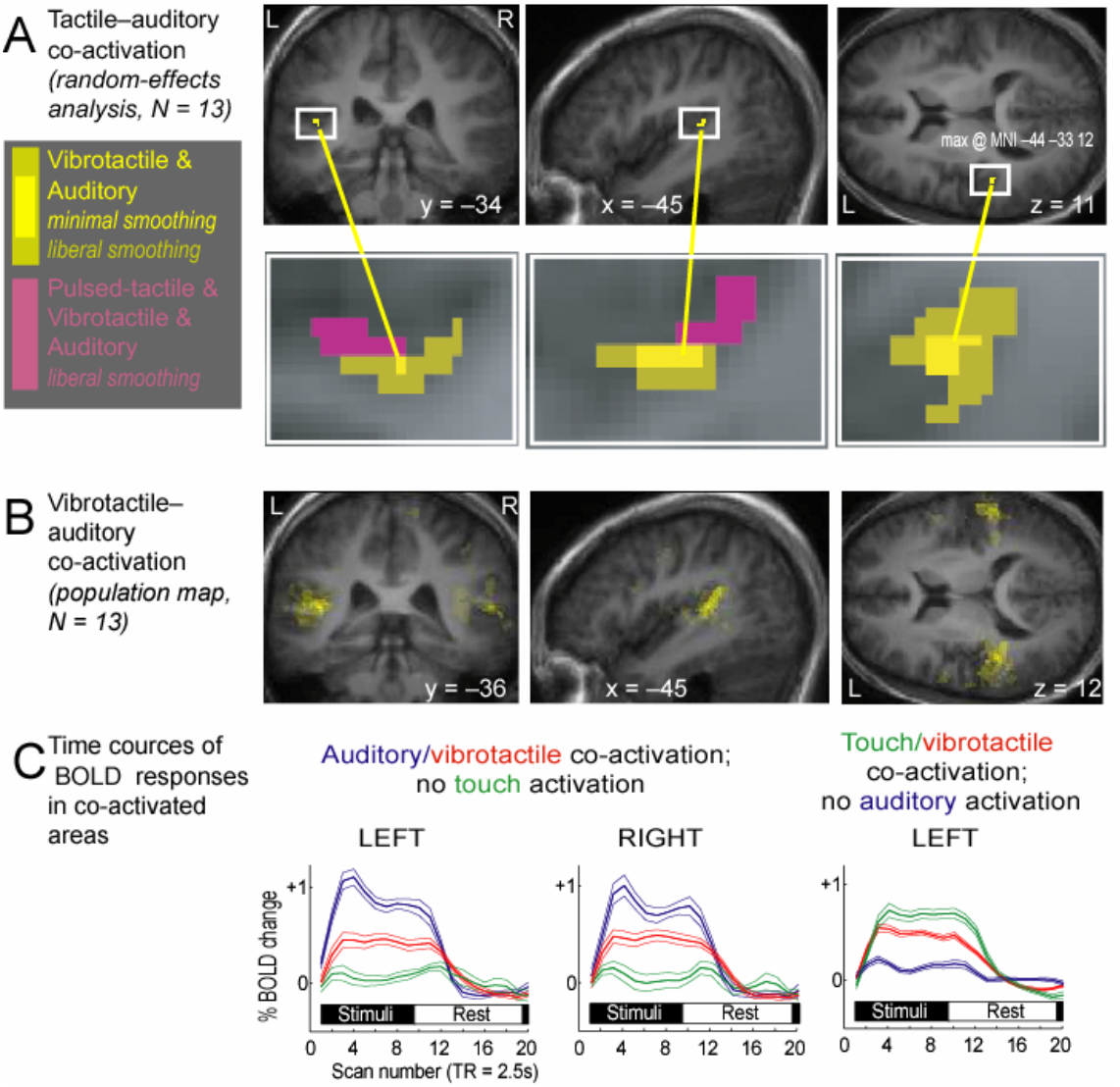

Figure 5.3 Study III

Panel A, upper row: vibrotactile–auditory co-activation (bright yellow) in the left superior temporal gyrus: a 19-voxel area of vibrotactile–auditory co-activation as obtained with minimal smoothing is shown. Enlarged views (lower row) show co-activated areas as obtained with liberal and minimal smoothing. **Panel B**, areas of vibrotactile–auditory co-activation are displayed as a population map across N = 13 subjects. **Panel C**, BOLD signal extracted from individual clusters of vibrotactile–auditory co-activation that did not show pulsed-tactile activation (shown here in the left row for the left hemisphere, mean ± SEM across N = 12 subjects, and in the middle row for the right hemisphere, N = 9 subjects) and for clusters of vibrotactile–pulsed-tactile co-activation that did not show auditory activation (right row). Adapted from Schürmann M, Caetano G, Hlushchuk Y, Jousmäki V, Hari R (2006) Touch activates human auditory cortex. *Neuroimage* 30: 1325-1331.

Individual subject analysis

Superimposing clusters obtained at individual level (with minimal smoothing) resulted in the population map, which showed vibrotactile–auditory co-activation in both hemispheres (Fig. 5.3B). Seven subjects contributed to the peak voxel (MNI −45 −36 12) in the left hemisphere, and five in the right hemisphere (MNI 66 −20 7).

An additional analysis step at the individual level served to identify clusters of voxels that were responsive to both vibrotactile and auditory stimuli but not to pulsed-tactile stimuli. In 9 out of 13 subjects, such clusters were found in both hemispheres. Fig. 5.3C (left and middle) shows average time courses of BOLD response for these clusters ($N = 12$ for the left hemisphere, and $N = 9$ for the right hemisphere). In both hemispheres, the activation is stronger to vibrotactile than auditory stimuli, and activation for pulsed-tactile stimuli is absent. The absence of tactile activation is not due to the low sensitivity of the method. To demonstrate this, Fig. 5.3C (right) shows BOLD signal time course for vibrotactile and pulsed-tactile co-activation (without auditory activation); such clusters were identified in all 13 subjects in the left hemisphere.

5.3.3 Discussion

The observed auditory–tactile co-activation confirms access of tactile input to the posterior auditory belt area. These findings are consistent with the intracranial recordings that documented responses of monkey auditory cortex to electrical median nerve stimuli (Schroeder et al., 2001), as well as to touch and vibration (Fu et al., 2003). An earlier fMRI study (Foxe et al., 2002) demonstrated that the response of the left superior temporal gyrus to the auditory–tactile stimulus pairs was stronger than the sum of responses to the stimuli presented alone. Interaction of auditory and tactile stimuli in MEG studies seemed, however, to suppress SII (Gobbele et al., 2003) and auditory cortex responses (Lütkenhöner et al., 2002).

Despite certain differences, the main results of Foxe et al. (2002) are consistent with our present findings, identifying the posterior auditory belt area of the left hemisphere as a region of tactile–auditory co-activation, consistent across subjects. Moreover, another study, which appeared when our paper was under revision, demonstrated with fMRI and electrophysiological recordings in anaesthetized monkeys auditory–tactile multisensory integration in the posterior auditory belt area (Kayser et al., 2005), same area as in our study.

As an extension to previous studies, we found that two types of tactile stimuli have access to the auditory belt area. Vibrotactile vs. pulsed-tactile differences in auditory cortex activation could be due to the temporal structure (frequency, similar to sounds) of the vibrotactile stimuli. Additionally, our results demonstrate that the apparent size of co-activation depends upon the spatial smoothing applied in the analysis.

The observed multisensory convergence could reflect processing of composite audiotactile events that arise during manual exploration of a texture or, more generally, during dynamic contact between hands and the environment.

5.4 Ipsilateral SI cortex is phasically suppressed during tactile finger stimulation (Study IV)

5.4.1 Experimental setup

This study comprised two experiments, with Experiment 2 designed on the basis of the results of Experiment 1.

In Experiment 1, tactile stimuli were delivered in random order to the index, middle, and ring fingers of the right hand, either at 1, 4, or 10 Hz in 25-s blocks. In Experiment 2, tactile stimuli were delivered unilaterally either to the left or right hand in separate blocks at frequencies from 1.7 to 5 Hz. The pseudorandomly arranged unilateral stimulation blocks alternated with rest blocks of the same duration.

To verify involvement of the SI cortex in the observed (in Experiment 1) deactivation, conjunction analysis of individual data was applied to detect regions in SI exhibiting tonic activation in response to contralateral tactile stimulation and phasic deactivation in response to ipsilateral stimulation. Furthermore, strict anatomical boundaries were imposed such that voxels were taken for SI (MI) activation only if they were active in an appropriate contrast and were located in the posterior (anterior) bank of the central sulcus. In the MI cortex we searched for regions exhibiting phasic deactivation to both left and right-sided unilateral stimulations. To avoid any smearing, which could impair exclusive localization of activations to the anterior or posterior bank of the central sulcus, no spatial smoothing was applied in the preprocessing of the fMRI data in Experiment 2.

5.4.2 Results

Areas responsive to tactile stimulation (Experiment 1)

Figure 5.4 (left) shows group-level activations during tactile stimulation. Positive BOLD responses (activations) are seen in the contralateral (left) SI cortex and in the SII region bilaterally. Statistically significant negative BOLD response (deactivation) appears in the ipsilateral (right) primary sensorimotor cortex. Additionally, a small activation

cluster is seen in the ipsilateral (right) SI, in the posterior wall of the postcentral gyrus, most likely in cytoarchitectonic area 2 (Grefkes et al., 2001).

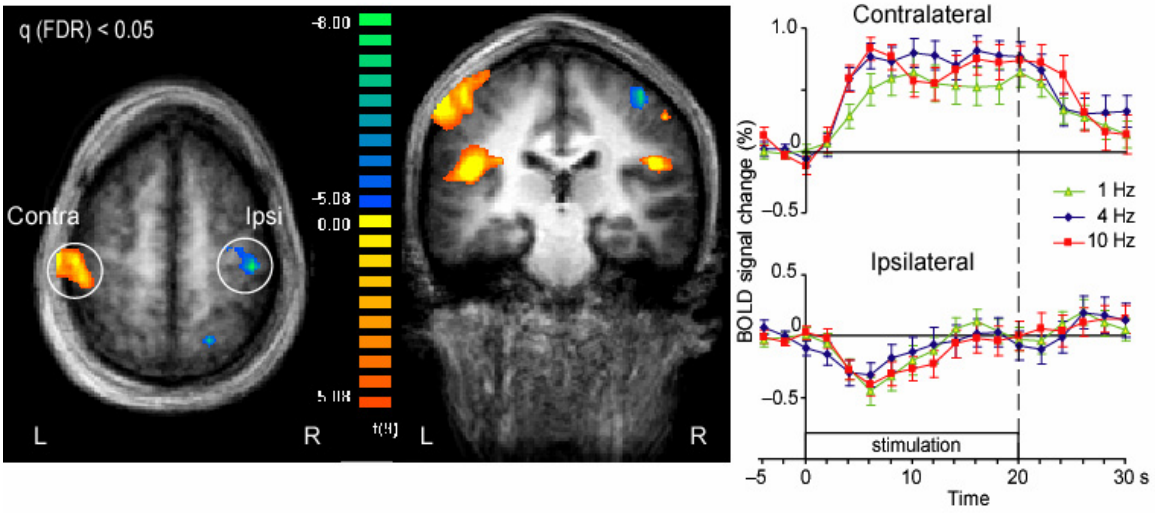

Figure 5.4 Study IV

Group-level analysis of activations to stimulation of right-hand fingertips in Experiment 1. Left: The statistical map overlaid onto the group average of Talairach-transformed anatomical images (N = 10). Contrast ([1Hz] + [4Hz] + [10Hz] – [baseline]) is shown at threshold of q(false discovery rate) < 0.05. In the color scale yellow and red refer to activations while blue and green refer to deactivations. Right: Mean ± SEM BOLD responses of 10 subjects in the contra- and ipsilateral rolandic cortex to right-hand stimulation. The different colors refer to different stimulation frequencies. Adapted from Hlushchuk Y, Hari R (2006) Transient suppression of ipsilateral primary somatosensory cortex during tactile finger stimulation. *J Neurosci* 26: 5819-5824.

Figure 5.4 (right) shows mean ± SEM (across 10 subjects) time courses of the BOLD responses in both SI cortices. In the contralateral SI region, the activation (positive BOLD response) lasts on average 45 s, clearly longer than the 25-s stimulation block. In contrast, a phasic deactivation (negative BOLD response) occurs in the ipsilateral SI cortex with an average duration of 18 s. The peak strength of the positive BOLD response in the contralateral SI cortex was 0.77 ± 0.19% (mean ± SEM, averaged across all 3 frequencies; $p < 0.001$ for deviation from zero level) and that of the ipsilateral negative BOLD response was –0.38 ± 0.17% ($p < 0.05$). Neither ipsilateral nor contralateral responses showed a clear difference between stimulation frequencies.

SI areas exhibiting negative BOLD response to ipsilateral stimuli (Experiment 2)

The BOLD responses observed in Experiment 1 had different time courses: the positive BOLD response outlasted the whole stimulation block whereas the negative BOLD response was phasic and returned to the baseline level already during the stimulation block. Therefore, for optimal detection of the BOLD responses, different

hemodynamic functions were used to model these two responses in Experiment 2 (see Fig. 5.5). The default hemodynamic response function in BV QX (Boynton et al., 1996) was used to model tonic, long-lasting responses whereas a custom-built model, based on the mean time course of the deactivation cluster in the ipsilateral rolandic cortex, was used to model phasic responses.

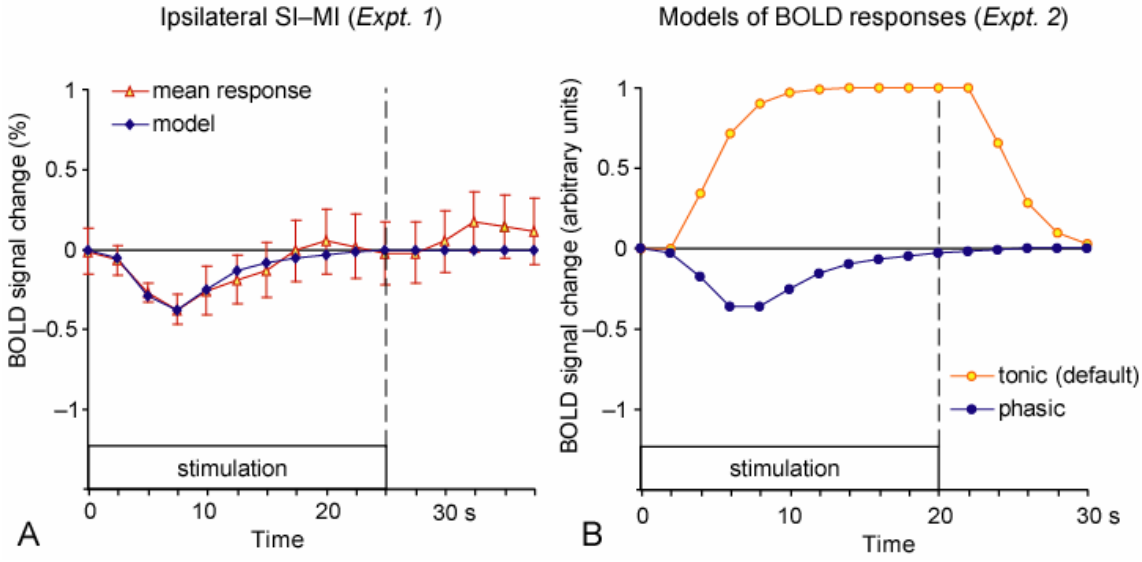

Figure 5.5 Study IV

Models used in Experiment 2. A (left): The mean ± SEM time course (n = 10) of the deactivation cluster (red symbols) and the phasic response model fitted to the data (blue line). B (right): Time courses of the two models: the tonic response model (orange; default in BV QX) and the custom-built phasic response model (blue). Note that the curves are sampled according to TR used: at 2.5-s intervals on the left (TR = 2.5 s in Experiment 1) and at 2-s intervals on the right (TR = 2 s in Experiment 2). Adapted from Hlushchuk Y, Hari R (2006) Transient suppression of ipsilateral primary somatosensory cortex during tactile finger stimulation. *J Neurosci* 26: 5819-5824.

The conjunction analysis was performed on individual data to reveal areas exhibiting sustained (canonical) positive BOLD responses to contralateral stimulation and phasic negative BOLD responses to ipsilateral stimulation.

Figure 5.6 (middle) shows, for one subject, brain regions that exhibit phasic negative BOLD response to ipsilateral stimulation and tonic positive BOLD response to contralateral stimulation. Areas fulfilling these criteria appear in both hemispheres in the SI cortex of the postcentral gyrus. We detected similar patterns in 7/10 subjects in the right SI cortex and in 7/10 in the left; while 5/10 subjects featured such patterns in both hemispheres.

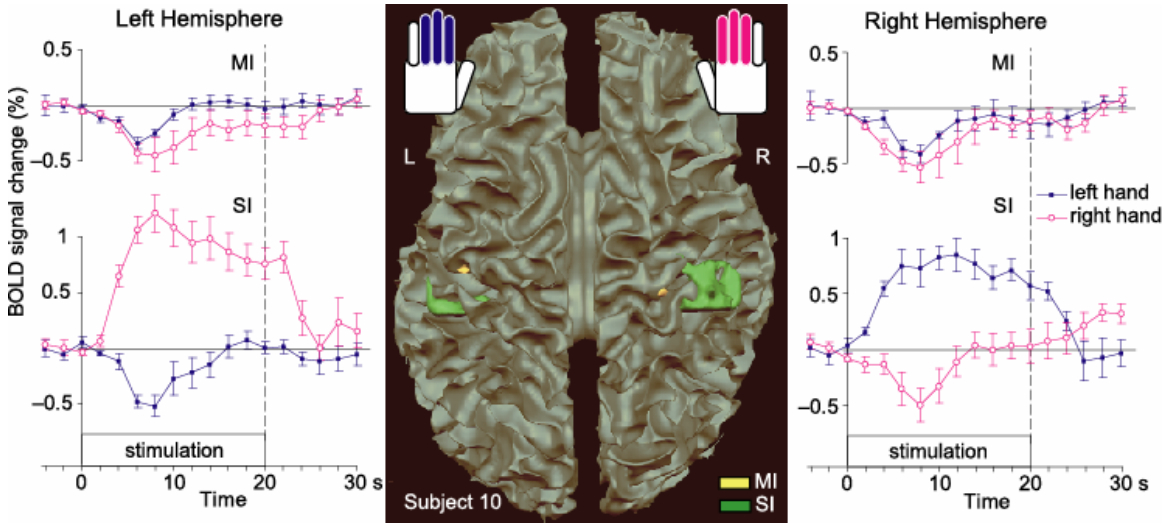

Figure 5.6 Study IV

Detected activation/deactivation regions in SI and MI cortices and time courses of those areas. Middle panel: The activation/deactivation clusters of Subject 10 are overlaid onto the white matter surface rendering. The yellow blobs show clusters in the MI and the green blobs in the SI cortices. Left and right panels: The traces show mean ± SEM BOLD response time courses of such clusters in the left and right hemispheres (N = 7 subjects for SI and N = 6 for MI). Adapted from Hlushchuk Y, Hari R (2006) Transient suppression of ipsilateral primary somatosensory cortex during tactile finger stimulation. *J Neurosci* 26: 5819-5824.

Figure 5.6 (outmost panels) shows the mean ± SEM BOLD responses for those subjects who have statistically significant clusters in the respective areas. Statistically significant positive BOLD changes to contralateral stimulation are seen in both hemispheres (peak amplitudes 0.84 ± 0.13% in the right SI, and 1.21 ± 0.16% in the left SI; both signals differ from zero at $p < 0.001$). Correspondingly, negative BOLD changes to ipsilateral stimulation are seen in these clusters (peak amplitudes -0.49 ± 0.15% in the right SI and –0.52 ± 0.15% in the left SI; both signals statistically significantly different from zero at $p < 0.01$).

Areas exhibiting negative BOLD response to both ipsilateral and contralateral stimulation (Experiment 2)

The contrast ([left hand] – baseline) + ([right hand] – baseline) demonstrated areas deactivated by both contralateral and ipsilateral stimulation. The detected areas in the anterior bank of the central sulcus (MI cortex) are depicted with yellow clusters in Figure 5.6 in both hemispheres of one subject. We detected similar patterns in the right hemisphere in 6/10 subjects and in 6/10 in the left, and 5 out of 10 subjects featured such pattern in both hemispheres. The mean ± SEM time courses of the negative BOLD responses in the MI cortices to both left and right unilateral stimulation are shown in the upper part of Figure 5.6.

Tactile stimuli to the right-hand fingers elicited negative BOLD response with a peak amplitude of –0.44 ± 0.15% ($p < 0.05$) in the left (contralateral) MI cortex and with a peak amplitude of –0.53 ± 0.20% ($p < 0.05$) in the right MI cortex. Correspondingly, stimulation of the left hand elicited negative BOLD responses in both left (-0.33 ± 0.03%; $p < 0.0001$) and right (-0.41 ± 0.03%; $p < 0.0001$) MI cortices.

5.4.3 Discussion

Our results demonstrate that unilateral tactile stimulation of fingers can be associated, in addition to the well-known activation of the contralateral SI cortex, with ipsilateral activation of postcentral sulcus (likely area 2) and deactivation of area 3b (in the ipsilateral SI cortex), as well as with deactivation of the MI cortex in both hemispheres. The elicited BOLD responses in the SI and MI cortices were tonic in case of activations and phasic in case of deactivations.

In fMRI, the BOLD signal has been demonstrated to correlate with the level of neuronal postsynaptic activity reflected in local field potentials (Logothetis et al., 2001; Mukamel et al., 2005; Niessing et al., 2005), suggesting that it primarily reflects neuronal input to the relevant cortical area and local processing rather than output activity (for a review, see Logothetis and Wandell, 2004). Hence an overall decrease of input and, accordingly, of neuronal activity in the studied brain area would appear as fMRI deactivation; according to the recently proposed mechanisms of neurovascular coupling, synaptic inhibition of cortical pyramidal cells in the area would also result in negative BOLD response (Lauritzen, 2005). With either approach, the negative BOLD response observed in our study is likely to result from neuronal inhibition of the area. Indeed, a recent study, published during the revision phase of our manuscript, demonstrated tight coupling between negative BOLD response and decreased neuronal activity in monkey VI cortex (Shmuel et al., 2006). The phasic time course of the negative BOLD response observed in our study (evident also in the pictures of Shmuel et al. (2006)) complements this interpretation, as inhibitory postsynaptic potentials attenuate quickly (Deisz and Prince, 1989) and may even disappear at high stimulus repetition rates (Nacimiento et al., 1964). Further supporting evidence comes from recent recordings of multiunit activity and local field potentials in alert macaque monkeys that demonstrated inhibition in area 3b in response to ipsilateral electrical median-nerve stimuli (Lipton et al., 2006).

The observed simultaneous activation of the contralateral SI and deactivation of the ipsilateral SI cortices could facilitate the left vs. right differentiation of touch during co-operative bilateral hand actions.

6 General Discussion

6.1 Representations of body parts in human somatosensory areas.

Mapping body part representations, particularly at the individual level, is crucial for evaluation of plastic changes; but prior to the investigation of such changes in individual body maps, general principles of body map organization in different human somatosensory areas need to be established. We attempted to characterize body part representations in somatosensory areas by means of MEG (I) and fMRI (II). Study I demonstrated distal-proximal arrangement to exist in human area 3b of the SI cortex. The obtained difference between representations of distal and proximal parts of the index finger was about 3 mm in the depth direction. Similar results (4 mm difference) were obtained in a concurrently published fMRI study (Blankenburg et al., 2003). Both studies could demonstrate the difference at group level, and even at the individual level such difference in the depth direction was observed in the majority of the subjects.

Study II demonstrated double representation of the fingers in the human SII region (3 submaxima were obtained with cardiac gating), consistent with previous fMRI findings (Disbrow et al., 2000; Ferretti et al., 2003; 2004). A recent anatomical study showed 4 cytoarchitectonic subdivisions of human SII region (Eickhoff et al., 2006a; 2006b). This finding suggested four different body maps within the SII region, a finding that neuroimaging studies have so far failed to support. Clarification of SII body maps is also obscured by strong heart-function-related movement in this region (Dagli et al., 1999). Cardiac-gated fMRI appeared useful for studying somatotopic representations in the SII cortex and thalamus—regions, compromised by the vicinity of comparatively large blood vessels: This technique has allowed us to detect body part representation more reliably at the individual level. A recent investigation regarding effectiveness of different cardiac-gated pulse sequences (Zhang et al., 2006) came to the same conclusion as in Study II: Cardiac-gating approaches are beneficial for selective investigation of regions with high pulsatile movement, like, e.g., the thalamus and brainstem.

6.2 How to overcome certain fMRI analysis pitfalls in tactile and cross-modality studies

Despite the improved results obtained using cardiac-triggered fMRI, Study II failed to recover somatotopic arrangement within the thalamus. Possibly, this challenging

task could be solved with a considerable increase of acquired time points and, correspondingly, of measurement time. The cardiac-gated fMRI has known drawbacks in time efficiency (only about half of the session time is used for the actual image acquisition). More time-efficient ways have been recently introduced to cardiac-triggered diffusion-weighted MR imaging by ordering slices in a particular manner (Nunes et al., 2005). Retrospective extraction of physiological noise from the acquired fMRI data (Biswal et al., 1996; Glover et al., 2000; Wang et al., 2005) would yield better time-efficiency than cardiac-triggered fMRI and a better SNR than conventional uncorrected fMRI. In contrast to BOLD fMRI employed in our studies, combination of imaging methods such as MRI and diffusion tractography, are now being introduced to delineate certain subunits of the thalamus, based on the anatomical structure and connectivity patterns (Behrens et al., 2003a; Johansen-Berg et al., 2005; Devlin et al., 2006). These methods succeeded to delineate major subunits of the thalamus, but no successful attempt to reveal somatotopic maps within the thalamus was reported.

Regarding issues of multisensory co-activation, the choice of smoothing parameters is crucial (White et al., 2001). Typical smoothing may over-estimate areas of co-activation but is essential in SPM analysis. On the other hand, minimal smoothing in our study has underestimated extent of vibrotactile–auditory co-activation due to subject-to-subject variability in the location of the co-activation. Such variability could also explain the lack of right-hemispheric vibrotactile–auditory co-activation in group analysis, despite the robust bilateral vibrotactile–auditory co-activation. Thus, in studies addressing co-activation of closely adjacent areas responsive to more than one type of stimulus, individual subject analysis with minimal or no smoothing proves to be an adequate approach. In contrast, group analysis typically assumes considerable smoothing and appears inadequate for such tasks.

We successfully applied a similar approach, individual subject analysis with no spatial smoothing, in Study IV. We exploited it to discriminate activations of closely adjacent areas such as SI and MI cortices on the opposing banks of the central sulcus (cf. auditory and SII cortex on the opposing banks of the lateral sulcus in Study III). The described individual level approach meets the demands of clinical applications: A conclusion should be made at individual level, since diagnosis involves single patients, not group averages.

6.3 Inhibition of ipsilateral SI cortex

Our estimated model of phasic negative BOLD response shows close similarity to the negative BOLD responses in macaque monkey VI cortex, demonstrated by Schmuel et al. (2006) to be tightly coupled with decreased neuronal activity in VI cortex. Moreover, recent intracortical recordings of multiunit activity and local field potentials in alert monkeys demonstrated inhibition in area 3b in response to ipsilateral electrical median nerve stimuli (Lipton et al., 2006). These finding allowed us to conclude, that the observed negative BOLD in ipsilateral area 3b is likely a result of interhemispheric inhibition.

One plausible explanation for the input to ipsilateral area 3b could be the following sequence (see Fig 6.1): Area 3b of the contralateral SI receives tactile input from fingers, and then—because of anteroposterior cortico-cortical projections—areas 1 and 2 of SI in the same hemisphere are activated as well. The ipsilateral SI could then obtain input through transcallosal connections, most likely via area 2 which has the densest transcallosal connections among all SI areas (Killackey et al., 1983) and was activated in our study. Instead, transcallosal connections in the hand representation of areas 3b are practically nonexistent in monkeys (Killackey et al., 1983), which precludes direct communication between 3b areas.

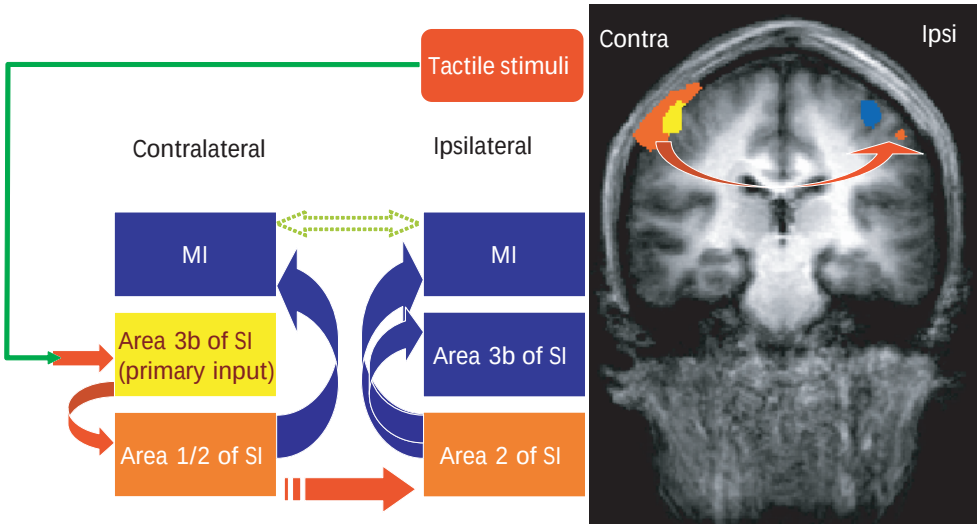

Figure 6.1 Study IV
A feasible model of how tactile input reaches ipsilateral area 3b (see detailed explanations in the text).

In accordance with the importance of transcallosal connections from area 2, it is important to note that in macaque monkeys, area 2 contains neurons with bilateral hand representations which depend on the transcallosal input from the contralateral SI (Iwamura

et al., 1994). Furthermore, area 2 also has reciprocal connections to area 3b and dense connections to the motor cortex (Yumiya and Ghez, 1984). These connections could be responsible for the observed deactivations in the ipsilateral area 3b and MI cortex. Furthermore, according to the suggested scheme (see Fig 5.6), the lack of area 2 neurons with bilateral receptive fields confined to the proximal forelimb (Iwamura et al., 1994) would explain why fMRI deactivation of the sensorimotor cortex has been observed for movements of distal but not proximal limbs (Nirkko et al., 2001). Recent optical neuroimaging findings (Tommerdahl et al., 2006), published soon after our paper, are in line with our results on ipsilateral input to the SI cortex. The authors of that study suggested involvement of interhemispheric connections between the SII cortices, which is not consistent with previous electrophysiological findings (Sutherland, 2006). These findings demonstrate that interaction of bimanual tactile stimuli occurs at the level of the SI cortex.

This thesis has demonstrated distal-proximal digit arrangement (I) and ipsilateral deactivation within area 3b (IV). Due to good reliability at the individual level, these features of area 3b are promising criteria for discriminating it from area 1. Reliable distinction between area 1 and area 3b would allow studies within individual functional areas of the SI cortex, in contrast to current labeling using vague anatomical landmarks. These findings provide powerful new tools for somatosensory research, analogous to methods using visual retinotopic maps to demarcate areas V1 and V2 in vision research.

7 Acknowledgements

I would like to give thanks to my wife, Irena and my supervisor, Prof. Riitta Hari in the first sentence, as their mutual respect and understanding was greatly beneficial for my peace-of-mind and, no doubt, for this thesis.

I would like to express my gratitude to Prof. Riitta Hari specifically for being brave enough to take me into the lab for the trial period which has smoothly extended into four years so far. It was my pleasure to do research under her soft and wise guidance for all those years, which I consider the best in my professional career.

I would like to acknowledge Ms. Gina Caetano, Doc. Nina Forss, Dr. Veikko Jousmäki, Ms. Sanna Malinen, Dr. Martin Schürmann, whose fruitful collaboration made this thesis possible. I thank Profs. Synnöve Carlson and Juhani Partanen, members of my follow-up group, for their advice and support. Dr. Mark Andermann, Doc. Nina Forss and Prof. Riitta Hari deserve special thanks for their precious comments in the preparation stage of this thesis.

I thank the reviewers of my thesis, Profs. Risto A. Kauppinen and Juhani Partanen, whose comments have improved it tremendously.

I would like to thank Dr. Cristina Simões-Franklin, Mr. Nuutti Vartiainen, and Ms. Marita Kattelus for active participation in the fMRI measurements, Ms. Jaana Hiltunen, Drs. Raimo Joensuu and Antti Tarkiainen for expert technical advice, and Drs. Jesper Andersson and Cyril Pernet for valuable discussions on fMRI analysis and numerous suggestions on how to reanalyze my data.

A lot of gratitude to Prof. Mikko Paalanen, who, in addition to being a nice boss, always showed vivid interest in the life of my home country, Ukraine. Many thanks go to Mss. Pirjo Muukkonen, Liisi Pasanen, Tuire Koivisto and Satu Pakarinen for taking care of bureaucracy issues and this way greatly simplifying my life in Finland that allowed me to pursue research issues in the lab full-time.

I sincerely thank everyone in the lab, current and previous employees, whom I have met, for creating this really enjoyable atmosphere for research and, even more, for social events. I am really grateful for the patient guidance in the jungles of Finnish language that I received on a daily basis mainly from the inhabitants of the corner room: Dr. Juha Järveläinen, Dr. Erika Kirveskari, Ms Satu Lamminmäki, Dr. Marjatta Pohja, Mr. Nuuti Vartiainen and Mr. Mikko Viinikainen.

I would like to thank my wife and kids (Katrina, Ksenia and Kaj) who patiently waited at home while their father was sitting in the office during numerous attempts to get the current thesis done, and my mother, who did her best to ease their waiting. I have also to mention with a good word my brothers, Dr. Yuriy Hlushchuk and Dr. Ruslan Hlushchuk, for patiently waiting, without teasing, for my PhD thesis.

The research incorporated into this thesis was carried out in the Brain Research Unit of Low Temperature Laboratory (LTL) and in the Advanced Magnetic Imaging centre (AMI), both at the Helsinki University of Technology, Espoo, Finland. Financially, the studies were supported by Academy of Finland (National Center of Excellence Program), the Ministry of Education Finland via the Finnish Graduate School of Neuroscience, Center for International Mobility, Finland, and by the Sigrid Jusélius Foundation.

References

Adrian ED (1940) Double representation of the feet in the sensory cortex of the cat. *J Physiol* 98: 16P-18P.

Ahonen AI, Hämäläinen MS, Kajola MJ, Knuutila JET, Laine PP, Lounasmaa OV, Simola JT, Tesche CD, Vilkman VA (1992) A 122-channel magnetometer covering the whole head. In: the 14th Annual International Conference of the IEEE Engineering in Medicine and Biology Society, Satellite Symposium on Neuroscience and Technology, pp 16-20. Lyon, France.

Allison JD, Meador KJ, Loring DW, Figueroa RE, Wright JC (2000) Functional MRI cerebral activation and deactivation during finger movement. *Neurology* 54: 135-142.

Allison T, McCarthy G, Wood CC, Williamson PD, Spencer DD (1989a) Human cortical potentials evoked by stimulation of the median nerve. II. Cytoarchitectonic areas generating long-latency activity. *J Neurophysiol* 62: 711-722.

Allison T, McCarthy G, Wood CC, Darcey TM, Spencer DD, Williamson PD (1989b) Human cortical potentials evoked by stimulation of the median nerve. I.Cytoarchitectonic areas generating short-latency activity. *J Neurophysiol* 62: 694-710.

Allison T, McCarthy G, Wood CC, Jones SJ (1991) Potentials evoked in human and monkey cerebral cortex by stimulation of the median nerve. A review of scalp and intracranial recordings. *Brain* 114: 2465-2503.

Allison T, McCarthy G, Luby M, Puce A, Spencer DD (1996) Localization of functional regions of human mesial cortex by somatosensory evoked potential recording and by cortical stimulation. *Electroencephalogr Clin Neurophysiol* 100: 126-140.

Attwell D, Iadecola C (2002) The neural basis of functional brain imaging signals. *Trends Neurosci* 25: 621-625.

Bandettini PA, Wong EC, Hinks RS, Tikofsky RS, Hyde JS (1992) Time course EPI of human brain function during task activation. *Magn Reson Med* 25: 390-397.

Bandettini PA, Wong EC (1995) Effects of biophysical and physiologic parameters on brain activation-induced changes: Simulations using a deterministic diffusion model. *International Journal of Imaging Systems and Technology* 6: 133-152.

Barkley GL, Baumgartner C (2003) MEG and EEG in epilepsy. *J Clin Neurophysiol* 20: 163-178.

Baule G, McFee R (1965) Theory of magnetic detection of the heart's electrical activity. *J Appl Phys* 36: 2066-2073.

Baumgartner C, Doppelbauer A, Sutherling WW, Zeitlhofer J, Lindinger G, Lind C, Deecke L (1991a) Human somatosensory cortical finger representation as studied by combined neuromagnetic and neuroelectric measurements. *Neurosci Lett* 134: 103-108.

Baumgartner C, Doppelbauer A, Deecke L, Barth DS, Zeitlhofer J, Lindinger G, Sutherling WW (1991b) Neuromagnetic investigation of somatotopy of human hand somatosensory cortex. *Exp Brain Res* 87: 641-648.

Behrens TE, Johansen-Berg H, Woolrich MW, Smith SM, Wheeler-Kingshott CA, Boulby PA, Barker GJ, Sillery EL, Sheehan K, Ciccarelli O, Thompson AJ, Brady JM, Matthews PM (2003a) Non-invasive mapping of connections between human thalamus and cortex using diffusion imaging. *Nat Neurosci* 6: 750-757.

Behrens TEJ, Woolrich MW, Jenkinson M, Johansen-Berg H, Nunes RG, Clare S, Matthews PM, Brady JM, Smith SM (2003b) Characterization and propagation of uncertainty in diffusion-weighted MR imaging. *Magn Res Med* 50: 1077-1088.

Biswal B, DeYoe AE, Hyde JS (1996) Reduction of physiological fluctuations in fMRI using digital filters. *Magn Reson Med* 35: 107-113.

Blankenburg F, Ruben J, Meyer R, Schwiemann J, Villringer A (2003) Evidence for a rostral-to-caudal somatotopic organization in human primary somatosensory cortex with mirror-reversal in areas 3b and 1. *Cereb Cortex* 13: 987-993.

Boynton GM, Engel SA, Glover GH, Heeger DJ (1996) Linear systems analysis of functional magnetic resonance imaging in human V1. *J Neurosci* 16: 4207-4221.

Buchner H, Adams L, Muller A, Ludwig I, Knepper A, Thron A, Niemann K, Scherg M (1995) Somatotopy of human hand somatosensory cortex revealed by dipole source analysis of early somatosensory evoked potentials and 3D-NMR tomography. *Electroencephalogr Clin Neurophysiol* 96: 121-134.

Buonomano DV, Merzenich MM (1998) Cortical plasticity: from synapses to maps. *Annu Rev Neurosci* 21: 149-186.

Burton H, Robinson CJ (1981) Organization of the S II parietal cortex: multiple somatic sensory representations within and near the second somatic sensory area of cynomolgus monkeys. In: Cortical sensory organization (Woolsey CN, ed), pp 67-120. Clifton, N.J.: Humana Press.

Burton H, MacLeod AM, Videen TO, Raichle ME (1997) Multiple foci in parietal and frontal cortex activated by rubbing embossed grating patterns across fingerpads: a positron emission tomography study in humans. *Cereb Cortex* 7: 3-17.
Caselli RJ (1991) Rediscovering tactile agnosia. *Mayo Clin Proc* 66: 129-142.
Caselli RJ (1993) Ventrolateral and dorsomedial somatosensory association cortex damage produces distinct somesthetic syndromes in humans. *Neurology* 43: 762-771.
Cohen D (1968) Magnetoencephalography: evidence of magnetic fields produced by alpha-rhythm currents. *Science* 161: 784-786.
Cohen D (1972) Magnetoencephalography: detection of the brain's electrical activity with a superconducting magnetometer. *Science* 175: 664-666.
Cohen D, Cuffin BN (1983) Demonstration of useful differences between magnetoencephalogram and electroencephalogram. *Electroencephalogr Clin Neurophysiol* 56: 38-51.
Cohen D, Cuffin BN (1987) A method for combining MEG and EEG to determine the sources. *Phys Med Biol* 32: 85-89.
Cohen D, Cuffin BN, Yunokuchi K, Maniewski R, Purcell C, Cosgrove GR, Ives J, Kennedy JG, Schomer DL (1990) MEG versus EEG localization test using implanted sources in the human brain. *Ann Neurol* 28: 811-817.
Cuffin BN, Cohen D (1979) Comparison of the magnetoencephalogram and electroencephalogram. *Electroencephalogr Clin Neurophysiol* 47: 132-146.
Culham JC, Valyear KF (2006) Human parietal cortex in action. *Curr Opin Neurobiol* 16: 205-212.
Dagli MS, Ingeholm JE, Haxby JV (1999) Localization of cardiac-induced signal change in fMRI. *Neuroimage* 9: 407-415.
DaSilva AF, Becerra L, Makris N, Strassman AM, Gonzalez RG, Geatrakis N, Borsook D (2002) Somatotopic activation in the human trigeminal pain pathway. *J Neurosci* 22: 8183-8192.
Davis KD, Kwan CL, Crawley AP, Mikulis DJ (1998) Functional MRI study of thalamic and cortical activations evoked by cutaneous heat, cold, and tactile stimuli. *J Neurophysiol* 80: 1533-1546.
Deisz RA, Prince DA (1989) Frequency-dependent depression of inhibition in guinea-pig neocortex in vitro by GABAB receptor feed-back on GABA release. *J Physiol* 412: 513-541.
Del Gratta C, Della Penna S, Tartaro A, Ferretti A, Torquati K, Bonomo L, Romani GL, Rossini PM (2000) Topographic organization of the human primary and secondary somatosensory areas: an fMRI study. *Neuroreport* 11: 2035-2043.
Del Gratta C, Della Penna S, Ferretti A, Franciotti R, Pizzella V, Tartaro A, Torquati K, Bonomo L, Romani GL, Rossini PM (2002) Topographic organization of the human primary and secondary somatosensory cortices: comparison of fMRI and MEG findings. *Neuroimage* 17: 1373-1383.
Deuchert M, Ruben J, Schwiemann J, Meyer R, Thees S, Krause T, Blankenburg F, Villringer K, Kurth R, Curio G, Villringer A (2002) Event-related fMRI of the somatosensory system using electrical finger stimulation. *Neuroreport* 13: 365-369.
Devlin JT, Sillery EL, Hall DA, Hobden P, Behrens TE, Nunes RG, Clare S, Matthews PM, Moore DR, Johansen-Berg H (2006) Reliable identification of the auditory thalamus using multi-modal structural analyses. *Neuroimage* 30: 1112-1120.
Disbrow E, Roberts T, Krubitzer L (2000) Somatotopic organization of cortical fields in the lateral sulcus of Homo sapiens: evidence for SII and PV. *J Comp Neurol* 418: 1-21.
Disbrow E, Roberts T, Poeppel D, Krubitzer L (2001) Evidence for interhemispheric processing of inputs from the hands in human S2 and PV. *J Neurophysiol* 85: 2236-2244.
Druschky K, Kaltenhauser M, Hummel C, Druschky A, Pauli E, Huk WJ, Stefan H, Neundorfer B (2002) Somatotopic organization of the ventral and dorsal finger surface representations in human primary sensory cortex evaluated by magnetoencephalography. *Neuroimage* 15: 182-189.
DuBois RM, Cohen MS (2000) Spatiotopic organization in human superior colliculus observed with fMRI. *Neuroimage* 12: 63-70.
Duong TQ, Kim DS, Ugurbil K, Kim SG (2001) Localized cerebral blood flow response at submillimeter columnar resolution. *Proc Natl Acad Sci U S A* 98: 10904-10909.
Eickhoff SB, Schleicher A, Zilles K, Amunts K (2006a) The human parietal operculum. I. Cytoarchitectonic mapping of subdivisions. *Cereb Cortex* 16: 254-267.
Eickhoff SB, Amunts K, Mohlberg H, Zilles K (2006b) The human parietal operculum. II. Stereotaxic maps and correlation with functional imaging results. *Cereb Cortex* 16: 268-279.
Elbert T, Pantev C, Wienbruch C, Rockstroh B, Taub E (1995) Increased cortical representation of the fingers of the left hand in string players. *Science* 270: 305-307.
Evans AC, Collins DL, Mills SR, Brown ED, Kelly RL, Peters TM (1993) 3D statistical neuroanatomical models from 305 MRI volumes. In: IEEE-Nuclear Science Symposium and Medical Imaging Conference, pp 1813-1817.

Feldman DE, Brecht M (2005) Map plasticity in somatosensory cortex. *Science* 310: 810-815.
Ferretti A, Babiloni C, Gratta CD, Caulo M, Tartaro A, Bonomo L, Rossini PM, Romani GL (2003) Functional topography of the secondary somatosensory cortex for nonpainful and painful stimuli: an fMRI study. *Neuroimage* 20: 1625-1638.
Ferretti A, Del Gratta C, Babiloni C, Caulo M, Arienzo D, Tartaro A, Rossini PM, Luca Romani G (2004) Functional topography of the secondary somatosensory cortex for nonpainful and painful stimulation of median and tibial nerve: an fMRI study. *Neuroimage* 23: 1217-1225.
Foerster O (1936) Sensible corticale Felder. In: Handbuch der Neurologie (Bumke O, Foerster O, eds), pp 358–448. Berlin: Julius Springer.
Fogassi L, Luppino G (2005) Motor functions of the parietal lobe. *Curr Opin Neurobiol* 15: 626-631.
Forss N, Salmelin R, Hari R (1994a) Comparison of somatosensory evoked fields to airpuff and electric stimuli. *Electroencephalogr Clin Neurophysiol* 92: 510-517.
Forss N, Hari R, Salmelin R, Ahonen A, Hämäläinen M, Kajola M, Knuutila J, Simola J (1994b) Activation of the human posterior parietal cortex by median nerve stimulation. *Exp Brain Res* 99: 309-315.
Forss N, Hietanen M, Salonen O, Hari R (1999) Modified activation of somatosensory cortical network in patients with right-hemisphere stroke. *Brain* 122: 1889-1899.
Fox PT, Burton H, Raichle ME (1987) Mapping human somatosensory cortex with positron emission tomography. *J Neurosurg* 67: 34-43.
Foxe JJ, Morocz IA, Murray MM, Higgins BA, Javitt DC, Schroeder CE (2000) Multisensory auditory-somatosensory interactions in early cortical processing revealed by high-density electrical mapping. *Brain Res Cogn Brain Res* 10: 77-83.
Foxe JJ, Wylie GR, Martinez A, Schroeder CE, Javitt DC, Guilfoyle D, Ritter W, Murray MM (2002) Auditory-somatosensory multisensory processing in auditory association cortex: an fMRI study. *J Neurophysiol* 88: 540-543.
Francis ST, Kelly EF, Bowtell R, Dunseath WJ, Folger SE, McGlone F (2000) fMRI of the responses to vibratory stimulation of digit tips. *Neuroimage* 11: 188-202.
Friston KJ, Jezzard P, R. T (1994) Analysis of functional MRI time-series. *Hum Brain Mapp* 1: 153-171.
Frot M, Mauguiere F (1999) Timing and spatial distribution of somatosensory responses recorded in the upper bank of the sylvian fissure (SII area) in humans. *Cereb Cortex* 9: 854-863.
Fu KM, Johnston TA, Shah AS, Arnold L, Smiley J, Hackett TA, Garraghty PE, Schroeder CE (2003) Auditory cortical neurons respond to somatosensory stimulation. *J Neurosci* 23: 7510-7515.
Fuchs M, Wagner M, Wischmann HA, Kohler T, Theissen A, Drenckhahn R, Buchner H (1998) Improving source reconstructions by combining bioelectric and biomagnetic data. *Electroencephalogr Clin Neurophysiol* 107: 93-111.
Garraghty PE, Pons TP, Kaas JH (1990) Ablations of areas 3b (SI proper) and 3a of somatosensory cortex in marmosets deactivate the second and parietal ventral somatosensory areas. *Somatosens Mot Res* 7: 125-135.
Gelnar PA, Krauss BR, Szeverenyi NM, Apkarian AV (1998) Fingertip representation in the human somatosensory cortex: an fMRI study. *Neuroimage* 7: 261-283.
Genovese CR, Lazar NA, Nichols T (2002) Thresholding of statistical maps in functional neuroimaging using the false discovery rate. *Neuroimage* 15: 870-878.
Gerardin E, Lehericy S, Pochon JB, Tezenas du Montcel S, Mangin JF, Poupon F, Agid Y, Le Bihan D, Marsault C (2003) Foot, hand, face and eye representation in the human striatum. *Cereb Cortex* 13: 162-169.
Geyer S, Schleicher A, Zilles K (1999) Areas 3a, 3b, and 1 of human primary somatosensory cortex. *Neuroimage* 10: 63-83.
Glover GH, Li TQ, Ress D (2000) Image-based method for retrospective correction of physiological motion effects in fMRI: RETROICOR. *Magn Reson Med* 44: 162-167.
Gobbele R, Schürmann M, Forss N, Juottonen K, Buchner H, Hari R (2003) Activation of the human posterior parietal and temporoparietal cortices during audiotactile interaction. *Neuroimage* 20: 503-511.
Goense JB, Logothetis NK (2006) Laminar specificity in monkey V1 using high-resolution SE-fMRI. *Magn Reson Imaging* 24: 381-392.
Grefkes C, Geyer S, Schormann T, Roland P, Zilles K (2001) Human somatosensory area 2: observer-independent cytoarchitectonic mapping, interindividual variability, and population map. *Neuroimage* 14: 617-631.
Griffiths TD, Uppenkamp S, Johnsrude I, Josephs O, Patterson RD (2001) Encoding of the temporal regularity of sound in the human brainstem. *Nat Neurosci* 4: 633-637.
Gross J, Timmermann L, Kujala J, Dirks M, Schmitz F, Salmelin R, Schnitzler A (2002) The neural basis of intermittent motor control in humans. *Proc Natl Acad Sci U S A* 99: 2299-2302.

Grynszpan F, Geselowitz DB (1973) Model studies of the magnetocardiogram. *Biophys J* 13: 911-925.
Guest S, Catmur C, Lloyd D, Spence C (2002) Audiotactile interactions in roughness perception. *Exp Brain Res* 146: 161-171.
Guimaraes AR, Melcher JR, Talavage TM, Baker JR, Ledden P, Rosen BR, Kiang NY, Fullerton BC, Weisskoff RM (1998) Imaging subcortical auditory activity in humans. *Hum Brain Mapp* 6: 33-41.
Haacke EM, Brown RW, Thompson MR, Venkatesan R (1999) Magnetic resonance imaging: physical principles and sequence design. New York: J. Wiley-Liss.
Hamzei F, Dettmers C, Rzanny R, Liepert J, Buchel C, Weiller C (2002) Reduction of excitability ("inhibition") in the ipsilateral primary motor cortex is mirrored by fMRI signal decreases. *Neuroimage* 17: 490-496.
Harel N, Ugurbil K, Uludag K, Yacoub E (2006) Frontiers of brain mapping using MRI. *J Magn Reson Imaging* 23: 945-957.
Hari R, Aittoniemi K, Jarvinen ML, Katila T, Varpula T (1980) Auditory evoked transient and sustained magnetic fields of the human brain. Localization of neural generators. *Exp Brain Res* 40: 237-240.
Hari R, Kaukoranta E, Reinikainen K, Huopaniemie T, Mauno J (1983a) Neuromagnetic localization of cortical activity evoked by painful dental stimulation in man. *Neurosci Lett* 42: 77-82.
Hari R, Hämäläinen M, Kaukoranta E, Reinikainen K, Teszner D (1983b) Neuromagnetic responses from the second somatosensory cortex in man. *Acta Neurol Scand* 68: 207-212.
Hari R, Reinikainen K, Kaukoranta E, Hämäläinen M, Ilmoniemi R, Penttinen A, Salminen J, Teszner D (1984) Somatosensory evoked cerebral magnetic fields from SI and SII in man. *Electroencephalogr Clin Neurophysiol* 57: 254-263.
Hari R (1990) The neuromagnetic method in the study of the human auditory cortex. In: Auditory Evoked Magnetic Fields and Electric Potentials (Grandori F, Hoke M, Romani GL, eds), pp 222-282. Basel: Karger.
Hari R, Hämäläinen M, Ilmoniemi R, Lounasmaa OV (1991) MEG versus EEG localization test. *Ann Neurol* 30: 222-223.
Hari R, Karhu J, Hämäläinen M, Knuutila J, Salonen O, Sams M, Vilkman V (1993) Functional organization of the human first and second somatosensory cortices: a neuromagnetic study. *Eur J Neurosci* 5: 724-734.
Hari R, Portin K, Kettenmann B, Jousmäki V, Kobal G (1997) Right-hemisphere preponderance of responses to painful CO2 stimulation of the human nasal mucosa. *Pain* 72: 145-151.
Hari R (1998) Magnetoencephalography as a tool of clinical neurophysiology. In: Electroencephalography: Basic Principles, Clinical Applications, and Related Fields, 4th Edition (Neidermeyer E, Lopes Da Silva F, eds), pp 1107–1134. Baltimore: Williams and Wilkins.
Hari R, Imada T (1999) Ipsilateral movement-evoked fields reconsidered. *Neuroimage* 10: 582-588.
Hari R, Forss N (1999) Magnetoencephalography in the study of human somatosensory cortical processing. *Philos Trans R Soc Lond B Biol Sci* 354: 1145-1154.
Hari R (2004) Magnetoencephalography in clinical neurophysiological assessment of human cortical functions. In: Electroencephalography: Basic Principles, Clinical Applications, and Related Fields, 5th Edition (Neidermeyer E, Lopes Da Silva F, eds), pp 1165–1197. Baltimore: Williams and Wilkins.
Hashimoto I, Mashiko T, Kimura T, Imada T (1999a) Are there discrete distal-proximal representations of the index finger and palm in the human somatosensory cortex? A neuromagnetic study. *Clin Neurophysiol* 110: 430-437.
Hashimoto I, Saito Y, Iguchi Y, Kimura T, Fukushima T, Terasaki O, Sakuma K (1999b) Distal-proximal somatotopy in the human hand somatosensory cortex: a reappraisal. *Exp Brain Res* 129: 467-472.
Hashimoto I, Kimura T, Iguchi Y, Takino R, Sekihara K (2001) Dynamic activation of distinct cytoarchitectonic areas of the human SI cortex after median nerve stimulation. *Neuroreport* 12: 1891-1897.
Huettel SA, Song AW, McCarthy G (2004) Functional magnetic resonance imaging. Sunderland, Mass.: Sinauer Associates Publishers.
Huttunen J, Kobal G, Kaukoranta E, Hari R (1986) Cortical responses to painful CO2 stimulation of nasal mucosa; a magnetoencephalographic study in man. *Electroencephalogr Clin Neurophysiol* 64: 347-349.
Hyvärinen J, Poranen A (1978) Receptive field integration and submodality convergence in the hand area of the post-central gyrus of the alert monkey. *J Physiol* 283: 539-556.
Hämäläinen M (1989) A 24-channel planar gradiometer: system design and analysis of neuromagnetic data. In: Advances in Biomagnetism (Williamson J, Hoke M, Stroink G, Kotani M, eds), pp 639-644. New York: Plenum Press.

Hämäläinen M, Hari R, Ilmoniemi RJ, Knuutila J, Lounasmaa OV (1993) Magnetoencephalography - theory, instrumentation, and applications to noninvasive studies of the working human brain. *Rev Mod Phys* 65: 413-497.

Iacoboni M (2006) Visuo-motor integration and control in the human posterior parietal cortex: Evidence from TMS and fMRI. *Neuropsychologia*.

Ilmoniemi R, Hari R, Reinikainen K (1984) A four-channel SQUID magnetometer for brain research. *Electroencephalogr Clin Neurophysiol* 58: 467-473.

Inui K, Wang X, Tamura Y, Kaneoke Y, Kakigi R (2004) Serial processing in the human somatosensory system. *Cereb Cortex* 14: 851-857.

Iwamura Y, Tanaka M, Hikosaka O (1980) Overlapping representation of fingers in the somatosensory cortex (area 2) of the conscious monkey. *Brain Res* 197: 516-520.

Iwamura Y, Tanaka M, Sakamoto M, Hikosaka O (1983a) Functional subdivisions representing different finger regions in area 3 of the first somatosensory cortex of the conscious monkey. *Exp Brain Res* 51: 315-326.

Iwamura Y, Tanaka M, Sakamoto M, Hikosaka O (1983b) Converging patterns of finger representation and complex response properties of neurons in area 1 of the first somatosensory cortex of the conscious monkey. *Exp Brain Res* 51: 327-337.

Iwamura Y, Tanaka M, Sakamoto M, Hikosaka O (1993) Rostrocaudal gradients in the neuronal receptive field complexity in the finger region of the alert monkey's postcentral gyrus. *Exp Brain Res* 92: 360-368.

Iwamura Y, Iriki A, Tanaka M (1994) Bilateral hand representation in the postcentral somatosensory cortex. *Nature* 369: 554-556.

Johansen-Berg H, Behrens TE, Sillery E, Ciccarelli O, Thompson AJ, Smith SM, Matthews PM (2005) Functional-anatomical validation and individual variation of diffusion tractography-based segmentation of the human thalamus. *Cereb Cortex* 15: 31-39.

Johnson KO, Yoshioka T, Vega-Bermudez F (2000) Tactile functions of mechanoreceptive afferents innervating the hand. *J Clin Neurophysiol* 17: 539-558.

Jones EG, Powell TP (1969) Connexions of the somatic sensory cortex of the rhesus monkey. II. Contralateral cortical connexions. *Brain* 92: 717-730.

Jones EG, Powell TP (1970) Connexions of the somatic sensory cortex of the rhesus monkey. III. Thalamic connexions. *Brain* 93: 37-56.

Jousmäki V, Hari R (1998) Parchment-skin illusion: sound-biased touch. *Curr Biol* 8: R190–R191.

Jueptner M, Weiller C (1995) Review: does measurement of regional cerebral blood flow reflect synaptic activity? Implications for PET and fMRI. *Neuroimage* 2: 148-156.

Kaas JH, Sur M, Nelson RJ, Merzenich MM (1981) The postcentral somatosensory cortex: multiple representations of the body in primates. In: Cortical sensory organization (Woolsey CN, ed), pp 29-46. Clifton, N.J.: Humana Press.

Kaas JH, Hackett TA, Tramo MJ (1999) Auditory processing in primate cerebral cortex. *Curr Opin Neurobiol* 9: 164.

Kajola M, Ahlfors S, Ehnholm GJ, Hälström J, Hämäläinen MS, Ilmoniemi RJ, Kiviranta M, Knuutila J, Lounasmaa OV, Tesche CD, Vilkman V (1989) A 24-channel magnetometer for brain research. In: Advances in Biomagnetism (Williamson J, Hoke M, Stroink G, Kotani M, eds), pp 673-676. New York: Plenum Press.

Kajola M, Ahonen A, Hamalainen MS, Knuutila J, Lounasmaa OV, Simola J, Vilkman V (1991) Development of multichannel neuromagnetic instrumentation in Finland. *Clin Phys Physiol Meas* 12 Suppl B: 39-44.

Kandel ER, Schwartz JH, Jessell TM (2000) Principles of neural science, 4th Edition. New York: McGraw-Hill Health Professions Division.

Kanno A, Nakasato N, Hatanaka K, Yoshimoto T (2003) Ipsilateral area 3b responses to median nerve somatosensory stimulation. *Neuroimage* 18: 169-177.

Karhu J, Tesche CD (1999) Simultaneous early processing of sensory input in human primary (SI) and secondary (SII) somatosensory cortices. *J Neurophysiol* 81: 2017-2025.

Karnath HO, Perenin MT (2005) Cortical control of visually guided reaching: evidence from patients with optic ataxia. *Cereb Cortex* 15: 1561-1569.

Kayser C, Petkov CI, Augath M, Logothetis NK (2005) Integration of touch and sound in auditory cortex. *Neuron* 48: 373-384.

Kelly AMC, Garavan H (2005) Human functional neuroimaging of brain changes associated with practice. *Cereb Cortex* 15: 1089-1102.

Killackey HP, Gould HJ, 3rd, Cusick CG, Pons TP, Kaas JH (1983) The relation of corpus callosum connections to architectonic fields and body surface maps in sensorimotor cortex of new and old world monkeys. *J Comp Neurol* 219: 384-419.

Knuutila J, Ahlfors S, Ahonen A, Hallstrom J, Kajola M, Lounasmaa OV, Vilkman V (1987) Large-area low-noise 7-channel DC SQUID magnetometer for brain research. *Rev Sci Instrum* 58: 2145-2156.

Korvenoja A, Wikström H, Huttunen J, Virtanen J, Laine P, Aronen HJ, Seppäläinen AM, Ilmoniemi RJ (1995) Activation of ipsilateral primary sensorimotor cortex by median nerve stimulation. *Neuroreport* 6: 2589-2593.

Korvenoja A, Huttunen J, Salli E, Pohjonen H, Martinkauppi S, Palva JM, Lauronen L, Virtanen J, Ilmoniemi RJ, Aronen HJ (1999) Activation of multiple cortical areas in response to somatosensory stimulation: combined magnetoencephalographic and functional magnetic resonance imaging. *Hum Brain Mapp* 8: 13-27.

Krause T, Kurth R, Ruben J, Schwiemann J, Villringer K, Deuchert M, Moosmann M, Brandt S, Wolf K, Curio G, Villringer A (2001) Representational overlap of adjacent fingers in multiple areas of human primary somatosensory cortex depends on electrical stimulus intensity: an fMRI study. *Brain Res* 899: 36-46.

Krubitzer LA, Kaas JH (1990) The organization and connections of somatosensory cortex in marmosets. *J Neurosci* 10: 952-974.

Krubitzer LA, Kaas JH (1992) The somatosensory thalamus of monkeys: cortical connections and a redefinition of nuclei in marmosets. *J Comp Neurol* 319: 123-140.

Krumbholz K, Schönwiesner M, Rübsamen R, Zilles K, Fink G, von Cramon Y (2005) Hierarchical processing of sound location and motion in the human brainstem and planum temporale. *Eur J Neurosci* 21: 230-238.

Kurth R, Villringer K, Mackert BM, Schwiemann J, Braun J, Curio G, Villringer A, Wolf KJ (1998) fMRI assessment of somatotopy in human Brodmann area 3b by electrical finger stimulation. *Neuroreport* 9: 207-212.

Kurth R, Villringer K, Curio G, Wolf KJ, Krause T, Repenthin J, Schwiemann J, Deuchert M, Villringer A (2000) fMRI shows multiple somatotopic digit representations in human primary somatosensory cortex. *Neuroreport* 11: 1487-1491.

Kwong KK, Belliveau JW, Chesler DA, Goldberg IE, Weisskoff RM, Poncelet BP, Kennedy DN, Hoppel BE, Cohen MS, Turner R, et al. (1992) Dynamic magnetic resonance imaging of human brain activity during primary sensory stimulation. *Proc Natl Acad Sci U S A* 89: 5675-5679.

Lauritzen M (2005) Reading vascular changes in brain imaging: is dendritic calcium the key? *Nat Rev Neurosci* 6: 77-85.

Lehericy S, van de Moortele PF, Lobel E, Paradis AL, Vidailhet M, Frouin V, Neveu P, Agid Y, Marsault C, Le Bihan D (1998) Somatotopical organization of striatal activation during finger and toe movement: a 3-T functional magnetic resonance imaging study. *Ann Neurol* 44: 398-404.

Levänen S, Jousmäki V, Hari R (1998) Vibration-induced auditory-cortex activation in a congenitally deaf adult. *Curr Biol* 8: 869-872.

Lin W, Kuppusamy K, Haacke EM, Burton H (1996) Functional MRI in human somatosensory cortex activated by touching textured surfaces. *J Magn Reson Imaging* 6: 565-572.

Lipton ML, Fu KM, Branch CA, Schroeder CE (2006) Ipsilateral hand input to area 3b revealed by converging hemodynamic and electrophysiological analyses in macaque monkeys. *J Neurosci* 26: 180-185.

Liu AK, Dale AM, Belliveau JW (2002) Monte Carlo simulation studies of EEG and MEG localization accuracy. *Hum Brain Mapp* 16: 47-62.

Logothetis NK, Pauls J, Augath M, Trinath T, Oeltermann A (2001) Neurophysiological investigation of the basis of the fMRI signal. *Nature* 412: 150-157.

Logothetis NK, Wandell BA (2004) Interpreting the BOLD signal. *Annu Rev Physiol* 66: 735-769.

Lopes da Silva FH, Wieringa HJ, Peters MJ (1991) Source localization of EEG versus MEG: empirical comparison using visually evoked responses and theoretical considerations. *Brain Topogr* 4: 133-142.

Lütkenhöner B, Lammertmann C, Simoes C, Hari R (2002) Magnetoencephalographic correlates of audiotactile interaction. *Neuroimage* 15: 509-522.

Maldjian JA, Gottschalk A, Patel RS, Detre JA, Alsop DC (1999) The sensory somatotopic map of the human hand demonstrated at 4 Tesla. *Neuroimage* 10: 55-62.

Mertens M, Lütkenhöner B (2000) Efficient neuromagnetic determination of landmarks in the somatosensory cortex. *Clin Neurophysiol* 111: 1478-1487.

Merzenich MM, Kaas JH, Sur M, Lin CS (1978) Double representation of the body surface within cytoarchitectonic areas 3b and 1 in "SI" in the owl monkey (Aotus trivirgatus). *J Comp Neurol* 181: 41-73.

Merzenich MM, Kaas JH, Wall J, Nelson RJ, Sur M, Felleman D (1983) Topographic reorganization of somatosensory cortical areas 3b and 1 in adult monkeys following restricted deafferentation. *Neuroscience* 8: 33-55.

Mima T, Nagamine T, Nakamura K, Shibasaki H (1998) Attention modulates both primary and second somatosensory cortical activities in humans: a magnetoencephalographic study. *J Neurophysiol* 80: 2215-2221.

Mogilner A, Grossman JA, Ribary U, Joliot M, Volkmann J, Rapaport D, Beasley RW, Llinas RR (1993) Somatosensory cortical plasticity in adult humans revealed by magnetoencephalography. *Proc Natl Acad Sci U S A* 90: 3593-3597.

Mukamel R, Gelbard H, Arieli A, Hasson U, Fried I, Malach R (2005) Coupling between neuronal firing, field potentials, and FMRI in human auditory cortex. *Science* 309: 951-954.

Murakami S, Okada Y (2006) Contributions of principal neocortical neurons to magnetoencephalography (MEG) and electroencephalography (EEG) signals. *J Physiol*.

Murray EA, Coulter JD (1981) Supplementary sensory area: the medial parietal cortex in the monkey. In: Cortical sensory organization (Woolsey CN, ed), pp 167-195. Clifton, N.J.: Humana Press.

Murray MM, Molholm S, Michel CM, Heslenfeld DJ, Ritter W, Javitt DC, Schroeder CE, Foxe JJ (2005) Grabbing your ear: rapid auditory-somatosensory multisensory interactions in low-level sensory cortices are not constrained by stimulus alignment. *Cereb Cortex* 15: 963-974.

Mäkelä JP, Ahonen A, Hämäläinen M, Hari R, Ilmoniemi R, Kajola M, Knuutila J, Lounasmaa OV, McEvoy L, Salmelin R, Salonen O, Sams M, Simola J, Tesche C, Vasama JP (1993) Functional differences between auditory cortices of the two hemispheres revealed by whole-head neuromagnetic recordings. *Hum Brain Mapp* 1: 48-56.

Nacimiento AC, Lux HD, Creutzfeldt OD (1964) Postsynaptic potentials of nerve cells of the motor cortex after electric stimulation of specific and nonspecific thalamic nuclei. *Pflugers Arch Gesamte Physiol Menschen Tiere* 281: 152-169.

Nelson RJ, Sur M, Felleman DJ, Kaas JH (1980) Representations of the body surface in postcentral parietal cortex of Macaca fascicularis. *J Comp Neurol* 192: 611-643.

Newton JM, Sunderland A, Gowland PA (2005) fMRI signal decreases in ipsilateral primary motor cortex during unilateral hand movements are related to duration and side of movement. *Neuroimage* 24: 1080-1087.

Niessing J, Ebisch B, Schmidt KE, Niessing M, Singer W, Galuske RA (2005) Hemodynamic signals correlate tightly with synchronized gamma oscillations. *Science* 309: 948-951.

Nihashi T, Naganawa S, Sato C, Kawai H, Nakamura T, Fukatsu H, Ishigaki T, Aoki I (2005) Contralateral and ipsilateral responses in primary somatosensory cortex following electrical median nerve stimulation—an fMRI study. *Clin Neurophysiol* 116: 842-848.

Nirkko AC, Ozdoba C, Redmond SM, Burki M, Schroth G, Hess CW, Wiesendanger M (2001) Different ipsilateral representations for distal and proximal movements in the sensorimotor cortex: activation and deactivation patterns. *Neuroimage* 13: 825-835.

Nitz DA (2006) Tracking route progression in the posterior parietal cortex. *Neuron* 49: 747-756.

Nudo RJ, Masterton RB (1986) Stimulation-induced [14C]2-deoxyglucose labeling of synaptic activity in the central auditory system. *J Comp Neurol* 245: 553-565.

Nunes RG, Jezzard P, Clare S (2005) Investigations on the efficiency of cardiac-gated methods for the acquisition of diffusion-weighted images. *J Magn Reson* 177: 102-110.

Nunez PL (1989) Estimation of large scale neocortical source activity with EEG surface Laplacians. *Brain Topogr* 2: 141-154.

Ogawa S, Lee TM, Kay AR, Tank DW (1990) Brain magnetic resonance imaging with contrast dependent on blood oxygenation. *Proc Natl Acad Sci U S A* 87: 9868-9872.

Ogawa S, Tank DW, Menon R, Ellermann JM, Kim SG, Merkle H, Ugurbil K (1992) Intrinsic signal changes accompanying sensory stimulation: functional brain mapping with magnetic resonance imaging. *Proc Natl Acad Sci U S A* 89: 5951-5955.

Ogawa S, Menon RS, Tank DW, Kim SG, Merkle H, Ellermann JM, Ugurbil K (1993) Functional brain mapping by blood oxygenation level-dependent contrast magnetic resonance imaging. A comparison of signal characteristics with a biophysical model. *Biophys J* 64: 803-812.

Okada YC, Tanenbaum R, Williamson SJ, Kaufman L (1984) Somatotopic organization of the human somatosensory cortex revealed by neuromagnetic measurements. *Exp Brain Res* 56: 197-205.

Okada YC, Wu J, Kyuhou S (1997) Genesis of MEG signals in a mammalian CNS structure. *Electroencephalogr Clin Neurophysiol* 103: 474-485.

Pascual-Leone A, Torres F (1993) Plasticity of the sensorimotor cortex representation of the reading finger in Braille readers. *Brain* 116: 39-52.
Penfield W, Boldrey E (1937) Somatotopic motor and sensory representation in the cerebral cortex of man as studied by electrical stimulation. *Brain* 60: 389–443.
Penfield W, Jasper HH (1954) Epilepsy and the functional anatomy of the human brain, [1st] Edition. Boston: Little Brown.
Pollok B, Gross J, Dirks M, Timmermann L, Schnitzler A (2004) The cerebral oscillatory network of voluntary tremor. *J Physiol* 554: 871-878.
Poncelet BP, Wedeen VJ, Weisskoff RM, Cohen MS (1992) Brain parenchyma motion: measurement with cine echo-planar MR imaging. *Radiology* 185: 645-651.
Pons TP, Garraghty PE, Mishkin M (1988) Lesion-induced plasticity in the second somatosensory cortex of adult macaques. *Proc Natl Acad Sci U S A* 85: 5279-5281.
Powell TP, Mountcastle VB (1959) Some aspects of the functional organization of the cortex of the postcentral gyrus of the monkey: a correlation of findings obtained in a single unit analysis with cytoarchitecture. *Bull Johns Hopkins Hosp* 105: 133-162.
Prado J, Clavagnier S, Otzenberger H, Scheiber C, Kennedy H, Perenin MT (2005) Two cortical systems for reaching in central and peripheral vision. *Neuron* 48: 849-858.
Purves D, Williams SM (2001) Neuroscience, 2nd Edition. Sunderland, Mass.: Sinauer Associates.
Rizzolatti G, Fogassi L, Gallese V (1997) Parietal cortex: from sight to action. *Curr Opin Neurobiol* 7: 562-567.
Robinson CJ, Burton H (1980) Organization of somatosensory receptive fields in cortical areas 7b, retroinsula, postauditory and granular insula of M. fascicularis. *J Comp Neurol* 192: 69-92.
Rossini PM, Pauri F (2000) Neuromagnetic integrated methods tracking human brain mechanisms of sensorimotor areas 'plastic' reorganisation. *Brain Res Brain Res Rev* 33: 131-154.
Ruben J, Schwiemann J, Deuchert M, Meyer R, Krause T, Curio G, Villringer K, Kurth R, Villringer A (2001) Somatotopic organization of human secondary somatosensory cortex. *Cereb Cortex* 11: 463-473.
Ruben J, Krause T, Taskin B, Blankenburg F, Moosmann M, Villringer A (2006) Sub-area-specific suppressive interaction in the BOLD responses to simultaneous finger stimulation in human primary somatosensory cortex: evidence for increasing rostral-to-caudal convergence. *Cereb Cortex* 16: 819-826.
Schnitzler A, Timmermann L, Gross J (2006) Physiological and pathological oscillatory networks in the human motor system. *J Physiol Paris* 99: 3-7.
Schroeder CE, Lindsley RW, Specht C, Marcovici A, Smiley JF, Javitt DC (2001) Somatosensory input to auditory association cortex in the macaque monkey. *J Neurophysiol* 85: 1322-1327.
Schürmann M, Caetano G, Jousmäki V, Hari R (2004) Hands help hearing: facilitatory audiotactile interaction at low sound-intensity levels. *J Acoust Soc Am* 115: 830-832.
Schönwiesner M, Krumbholz K, Fink G, Rübsamen R, von Cramon Y (2003) Binaural interaction in the human auditory cortex and subcortical structures. *NeuroImage* 19: S64.
Sherrick CE (1984) Basic and applied research on tactile aids for deaf people: Progress and prospects. *J Acoust Soc Am* 75: 1325.
Shmuel A, Yacoub E, Pfeuffer J, Van de Moortele PF, Adriany G, Hu X, Ugurbil K (2002) Sustained negative BOLD, blood flow and oxygen consumption response and its coupling to the positive response in the human brain. *Neuron* 36: 1195-1210.
Shmuel A, Augath M, Oeltermann A, Logothetis NK (2006) Negative functional MRI response correlates with decreases in neuronal activity in monkey visual area V1. *Nat Neurosci* 9: 569-577.
Smith AT, Singh KD, Greenlee MW (2000) Attentional suppression of activity in the human visual cortex. *Neuroreport* 11: 271-277.
Smith AT, Williams AL, Singh KD (2004) Negative BOLD in the visual cortex: evidence against blood stealing. *Hum Brain Mapp* 21: 213-220.
Stefanovic B, Warnking JM, Pike GB (2004) Hemodynamic and metabolic responses to neuronal inhibition. *Neuroimage* 22: 771-778.
Stevens RT, London SM, Apkarian AV (1993) Spinothalamocortical projections to the secondary somatosensory cortex (SII) in squirrel monkey. *Brain Res* 631: 241-246.
Sutherland MT (2006) The hand and the ipsilateral primary somatosensory cortex. *J Neurosci* 26: 8217-8218.
Tamura K (1972) Ipsilateral somatosensory evoked responses in man. *Folia Psychiatr Neurol Jpn* 26: 83-94.
Thulborn KR, Waterton JC, Matthews PM, Radda GK (1982) Oxygenation dependence of the transverse relaxation time of water protons in whole blood at high field. *Biochim Biophys Acta* 714: 265-270.

Timmermann L, Gross J, Dirks M, Volkmann J, Freund HJ, Schnitzler A (2003) The cerebral oscillatory network of parkinsonian resting tremor. *Brain* 126: 199-212.

Tommerdahl M, Simons SB, Chiu JS, Favorov O, Whitsel BL (2006) Ipsilateral input modifies the primary somatosensory cortex response to contralateral skin flutter. *J Neurosci* 26: 5970-5977.

Turman AB, Ferrington DG, Ghosh S, Morley JW, Rowe MJ (1992) Parallel processing of tactile information in the cerebral cortex of the cat: effect of reversible inactivation of SI on responsiveness of SII neurons. *J Neurophysiol* 67: 411-429.

Vallar G (1998) Spatial hemineglect in humans. *Trends in Cognitive Sciences* 2: 87-97.

Wang SJ, Luo LM, Liang XY, Gui ZG, Chen CX (2005) Estimation and removal of physiological noise from undersampled multi-slice fMRI data in image space. In: 27th International Annual Conference of the Engineering in Medicine and Biology Society, pp 1371-1373. Shanghai, China.

Ward NS, Brown MM, Thompson AJ, Frackowiak RS (2006) Longitudinal changes in cerebral response to proprioceptive input in individual patients after stroke: an FMRI study. *Neurorehabil Neural Repair* 20: 398-405.

Weisenberger JM, Miller JD (1987) The role of tactile aids in providing information about acoustic stimuli. *J Acoust Soc Am* 82: 906-916.

White T, O'Leary D, Magnotta V, Arndt S, Flaum M, Andreasen NC (2001) Anatomic and functional variability: the effects of filter size in group fMRI data analysis. *Neuroimage* 13: 577-588.

Williamson SJ (1991) MEG versus EEG localization test. *Ann Neurol* 30: 222-222.

Woolsey CN, Marshall WH, Bard P (1942) Representation of cutaneous tactile sensibility in the cerebral cortex of the monkey as indicated by evoked potentials. *Bull Johns Hopkins Hosp* 70: 399–441.

Young JP, Herath P, Eickhoff S, Choi J, Grefkes C, Zilles K, Roland PE (2004) Somatotopy and attentional modulation of the human parietal and opercular regions. *J Neurosci* 24: 5391-5399.

Yumiya H, Ghez C (1984) Specialized subregions in the cat motor cortex: anatomical demonstration of differential projections to rostral and caudal sectors. *Exp Brain Res* 53: 259-276.

Zhang HQ, Murray GM, Turman AB, Mackie PD, Coleman GT, Rowe MJ (1996) Parallel processing in cerebral cortex of the marmoset monkey: effect of reversible SI inactivation on tactile responses in SII. *J Neurophysiol* 76: 3633-3655.

Zhang HQ, Zachariah MK, Coleman GT, Rowe MJ (2001a) Hierarchical equivalence of somatosensory areas I and II for tactile processing in the cerebral cortex of the marmoset monkey. *J Neurophysiol* 85: 1823-1835.

Zhang HQ, Murray GM, Coleman GT, Turman AB, Zhang SP, Rowe MJ (2001b) Functional characteristics of the parallel SI- and SII-projecting neurons of the thalamic ventral posterior nucleus in the marmoset. *J Neurophysiol* 85: 1805-1822.

Zhang WT, Mainero C, Kumar A, Wiggins CJ, Benner T, Purdon PL, Bolar DS, Kwong KK, Sorensen AG (2006) Strategies for improving the detection of fMRI activation in trigeminal pathways with cardiac gating. *Neuroimage*.

Zilles K, Palomero-Gallagher N (2001) Cyto-, myelo-, and receptor architectonics of the human parietal cortex. *Neuroimage* 14: S8-20.

Zimmerman JE, Silver AH (1966) Macroscopic quantum interference effects through superconducting point contacts. *Phys Rev* 141: 367.

Zimmerman JE, Frederick NV (1971) Miniature ultrasensitive superconducting magnetic gradiometer and its use in cardiography and other applications. *Appl Phys Lett* 19: 16.